4-13-2015 12:00 AM

Abnormal Hippocampal Activation In Freely Behaving Mice Deficient For The Vesicular Acetylcholine Transporter

Shahin Moallem
The University of Western Ontario

Supervisor
Dr. Stan Leung
The University of Western Ontario

Graduate Program in Neuroscience
A thesis submitted in partial fulfillment of the requirements for the degree in Master of Science

Abnormal Hippocampal Activation In Freely Behaving Mice Deficient For The Vesicular Acetylcholine Transporter

(Thesis format: Monograph)

by

Shahin Moallem

Graduate Program in Neuroscience

A thesis submitted in partial fulfillment
of the requirements for the degree of
Masters of Science

The School of Graduate and Postdoctoral Studies
The University of Western Ontario
London, Ontario, Canada

Abstract

Acetylcholine (Ach) has a fundamental role in cortical activation. The activation of the hippocampus, a cortex implicated in cognitive and sensorimotor functions, is characterized by an increase in power and frequency of oscillations in the theta (4-10 Hz) and gamma (30-100 Hz) frequency range. We studied hippocampal activation in two mutant mouse lines with deficiency in cholinergic functionality: VAChT KD^{HET} (HET), and $VAChT^{Nkx2.1\text{-}Cre\text{-}flox/flox}$ (KO). We hypothesized that the mutant mice, relative to wild-type (WT) mice, will manifest abnormal theta and gamma oscillations during different behaviors, and in response to muscarinic cholinergic antagonist scopolamine hydrochloride and to the NMDA receptor glutamatergic antagonist CPP. Local field potentials (LFPs) were recorded from CA1 stratum radiatum in behaving WT and mutant mice before and after injection of drugs. Immobile theta power decreased in the order of WT, HET, and KO. Injection of scopolamine abolished the awake-immobility theta in WT and KO mice, but a theta peak remained in the HET mutant mice. Injection of CPP abolished the awake-immobility theta in HET mice but not in WT and KO mice. Our data suggests that acetylcholine is critical for immobile theta power. The presence of a scopolamine-resistant and CPP-sensitive theta rhythm during awake-immobility in HET mice is a novel finding, since immobility-associated theta rhythm was found to be scopolamine (or atropine) sensitive in WT mice and other laboratory animals. The compensatory changes that activate a scopolamine-resistant, presumably non-cholinergic, theta rhythm during immobility in HET mice remain to be identified.

KEYWORDS: acetylcholine, hippocampus, theta rhythm, gamma rhythm, scopolamine, CPP

Acknowledgments

I like to express my deepest gratitude to my supervisor Dr. Stan Leung for his patience, excellent guidance and support throughout the course of my graduate education. I like to thank my advisory committee members, Drs. Stefan Everling, Vania F. Prado and Paul Gribble.

I like to thank all of my lab members for their support and assistance. In particular, I would like to extend my appreciation specifically to Min-Ching Kuo and Justin Arcaro for their patience in teaching me the necessary skills to conduct electrode implantation surgery. I am especially grateful to our lab technician Liangwei Chu for preparing my electrodes and helping me in performing histology. I would like to thank Dr. Jingyi Ma for her essential help during my data analysis.

Table of Contents

List of Figures

List of Abbreviations

ACh	acetylcholine
AChE	acetylcholinesterase
AD	Alzheimer's disease
AMPA	2-amino-3-(5-methyl-3-oxo-1,2-oxazol-4-yl) propanoic acid
ANOVA	analysis of variance
CA(1-4)	Cornu Amonis
CaMKII	α-cal-calcium-calmodulin-dependent proteinkinase II
CSD	current source density
ChAT	choline acetyltransferase
CPP	3-[(R)-2-carboxypiperazin-4-yl]-prop-2-enyl-1-phosphonic acid
DBB	diagonal band of Broca
DHPG	(S)-3,5-dihyroxyphenylglycine
GABA	gamma aminobutyric acid
Hz	hertz
i.p.	intraperitoneal
kg	kilogram
LIA	large amplitude irregular activity
LFP	local field potentials
LTD	long term depression

LTP	long-term potentiation
mAChR	muscarinic acetylcholine receptor
mg	milligram
mGluR	metabotropic glutamate receptors
ml	milliliter
msec	milliseconds
MPO	membrane potential oscillations
MRI	magnetic resonance imaging
MS	medial septum
nAChR	nicotinic acetylcholine receptor
NMDA	N-methyl-D-aspartate
PLCß1	phospholipase C-ß1
PNO	pontis nucleus oralis
PH	posterior hypothalamic nucleus
PPT	pedunculopontine tegmental nucleus
REM	rapid eye movement
RPO	reticularis pontis oralis
RSA	rhythmical slow-wave activity
SEM	standard error of the mean
SUM	supramammilary nucleus

VAChT	vesicular acetylcholine transporter
VGLUT	vesicular glutamate transporter

1 Introduction

1.1 Hippocampus

The hippocampus is part of the limbic system located in the medial temporal lobe of the human brain and plays important roles in the consolidation of information from short-term memory to long-term memory and in spatial navigation.

1.1.1 Anatomy and circuitry of hippocampus

The hippocampus is one of the most studied brain areas in part due to its unique anatomy. The hippocampus in humans has been divided into six segments: dentate gyrus, cornu amonis (CA1-4) and the subiculum (Amaral and Witter, 1989). In rodents, CA4 is referred to as dentate hilus (Knowles, 1992). Hippocampal neurons and their projections have been organized in four layers. Stratum oriens is the most superficial layer followed by stratum pyramidale, stratum radiatum, and stratum lacunosum-moleculare (Amaral and Witter, 1989).

Pyramidal cells and granule cells are the two redundant cells found within the hippocampus. Pyramidal cells are located in cornu amonis regions (CA1, CA2, and CA3). Granule cells are found in the dentate gyrus, with their cell bodies located within stratum granulosum and their single dendritic arbour projecting to the molecular layer (Knowles, 1992). Dentate gyrus receives inputs from entorhinal cortex via the perforant pathway (Amaral and Witter, 1989; Anderson et al., 1971). Axons of the granule cells form the mossy fibers and innervate the proximal dendrites of the CA3 pyramidal cells in

stratum lucidum. Triangular shaped cell bodies of the CA1 pyramidal cells are located in the stratum pyramidale (Knowles, 1992). Basal and apical dendrites of the CA1 pyramidal cells are located in the stratum oriens and stratum radiatum respectively. Schaffer collaterals (axons of the CA3 pyramidal cells) innervate both basal and apical dentrites of CA1 pyramidal cells via commissural and associational paths (Buzaki and Eidelberg, 1992). Both CA1 and CA3 regions of hippocampus also receive inputs from enthornial cortex (Amaral and Witter, 1989). Axons of the CA1 pyramidal cells terminate at subiculum and enthornial cortex.

1.1.2 Interneurons

More than 20 types of interneurons have been classified that mostly use γ–aminobutyric acid (GABA) as a neurotransmitter (Freund and Buzsaki, 1996; Benes and Berretta, 2001; Klausberger and Somogyi, 2008). The four main types of interneurons are bistratified cells, basket cells, chandelier cells, and oriens–lacunosum moleculare (O-LM) interneurons. Bistratified cells innervate both apical and basal dendritic branches of the pyramidal cells (Benes and Berretta, 2001). Bistratified interneurons receive input from CA3 and may participate in generation of CA3-driven gamma oscillation (Tukker et al., 2007). Basket cells predominantly project to the cell body of pyramidal cells (Benes and Berretta, 2001). Basket cells burst at theta frequency (4-10Hz), with gamma frequency (30-100Hz) firing occurring within the bursts (Penttonen et al., 1998). Chandelier cells (also known as axo-axonic cells) form axo-axonic synapses with the initial segment of axons and regulate their action potential generation (Benes and Berretta, 2001). The oriens–lacunosum moleculare (O-LM) interneurons target the apical dendritic tuft aligned

with the entorhinal cortical input (Klausberger and Somogyi, 2008). Firing rate of interneurons may change with the behavior of an animal (Ranck, 1973).

1.2 Acetylcholine

Acetylcholine (ACh) in the nervous system has key functions in life, as it regulates multiple central and peripheral nervous system outputs. Acetylcholine is synthesized in the cytoplasm from acetyl-coenzyme A (derived from pyruvate generated in glycolysis within the mitochondria) and choline (Dobransky and Rylett, 2005). The reaction of choline with acetyl-CoA is catalyzed by an enzyme named choline acetyltransferase (ChAT) (Dobransky and Rylett, 2005). Synthesized ACh gets stored within the vesicles via a protein named vesicular acetylcholine transporter (VAChT). Upon arrival of action potentials, ACh is released into the synaptic cleft by exocytosis and then it gets degraded via a hydrolytic enzyme named actetylcholinesterase (AChE).

1.2.1 Cholinergic receptors

Muscarinic and nicotinic receptors are the two types of receptors classified for ACh. Muscarinic receptors are G-protein coupled receptors, and are divided into five subtypes (M1-M5). A broad range of muscarinic acetylcholine receptors (mAChRs) are expressed within the hippocampus, with M1, M3 and M5 receptors being mainly expressed postsynaptically on the pyramidal and granular cells and M2 and M4 receptors on the interneurons (Levey et al., 1995). M2 receptors also exist presynaptically on the cholinergic neurons projecting from medial septum to the hippocampus and play an auto-regulatory role (Rouse et al., 1999). Activation of mAChRs in the hippocampus modulates the activity of multiple ligand-gated receptors including *N*-methyl-D-aspartate

(NMDA) glutamatergic receptors of the pyramidal cells (Markram and Segal, 1990). In addition, activation of mAChRs directly excites GABAergic interneurons. At the same time, it has a depressant effect on the synaptic release of GABA (Cobb and Davis, 2005). Nicotinic acetylcholine receptors (nAChRs) are made up of a pentametric combination of α (α2-α10) and ß (ß2-ß4) subunits. In particular, α7 nAChR subtype is highly expressed in both glutamatergic and GABAergic axon terminals and postsynaptic sites (Fabian-Fine et al., 2001).

1.2.2 Acetylcholine and long term potentiation

Long term potentiation (LTP) in the hippocampus is proposed to model a neuronal mechanism of learning and memory formation (Bliss and Collingridge, 1993). There is evidence that enhancement of septohippocampal cholinergic activity in behaving mice via stimulation enhances long term potentiation (Galey et al., 1994). The level of acetylcholine released from terminals varies based on the behavior of the animal (Dudar et al., 1979). In behaving rats, release of ACh is highest during walking and rapid eye movement (REM) sleep (Dudar et al., 1979). While the animal is alert-immobile, release of ACh reduces and the least amount of ACh is released during slow wave sleep (Dudar et al., 1979). Hippocampal LTP was facilitated when induced during walking, as opposed to when induced in the absence of theta (i.e. immobility). In addition, systemic scopolamine or 192 IgG-saporin septal lesions or specific M1 receptor antagonist pirenzepine attenuated LTP induced during walking without affecting LTP induced during immobility (Leung et al., 2003).

Ji et al. (2001) reported that activation of presynaptic α7 nAChRs leads to an enhancement of glutamate release which increases the possibility of inducing LTP. On

the other hand, activation of α7 nAChRs on hippocampal interneurons can block LTP in the pyramidal cells (Ji et al., 2001). Activation of septo-hippocapal cholinergic neurons via optogenetics or electrical stimulation induced different types of hippocampal Schaeffer collateral to CA1 synaptic plasticity (Gu and Yekel, 2011). Such plasticity depended on the timing of cholinergic input relative to the Schaeffer collateral input (Gu and Yekel, 2011). An α7 nAChR-dependent LTP was induced when the cholinergic input was activated 100 or 10 msec prior to Schaeffer collateral stimulation while the cholinergic stimulation delayed until 10 msec after the Schaeffer collateral stimulation induced a mAChR-dependent LTP was induced (Gu and Yekel, 2011).

1.2.3 Alzheimer's disease and the cholinergic neurons

Alzheimer's disease (AD) is an age-dependent neurodegenerative disorder characterized by progressive dementia (Chen et al., 2011). Alzheimer's disease can be classified into three stages: 1) an early stage characterized by an inability to remember novel information where the initial encoding of that information is affected but not the retrieval of previously learned information; 2) a middle stage where deficits in semantic memory, working memory, spatial orientation, and attention are especially observed; and 3) a late stage (or dementia) characterized by a global intellectual breakdown associated with changes in personality and behavior (Bontempi et al., 2001).

It has been hypothesized that cholinergic dysfunction is a major cause for the cognitive deficit in AD (Bartus et al., 1982). Synthesis of ACh via choline acetyltransferase has been found to be decreased in the AD brain (Fisher, 2008). In addition, presynaptic cholinergic axonal loss can be identified by reduction of vesicular

acetylcholine transporter (Chen et al., 2011). Degeneration of cholinergic neurons in the basal forebrain that project to the hippocampus and cerebral cortex is evident in AD (Fisher, 2008). Using magnetic resonance imaging (MRI) and voxel-based morphometry (VBM). Teipel et al. (2005) found a positive correlation between stages of AD and reduction of cholinergic neurons of basal forebrain. This positive correlation may be due to the interaction between amyloid ß accumulation and cholinergic dysfunction (Schliebs et al., 2006). The most common prescribed medications to AD patients are the cholinesterase inhibitors such as Donepezil (Fisher, 2008).

1.3 Glutamate

Glutamate is the most abundant excitatory neurotransmitter in the vertebrate central nervous system (Meldrum, 2000). Similar to ACh, glutamate must be released from synaptic vesicles and the transport of glutamate into vesicles is mediated by vesicular glutamate transporter (VGLUT). To date, three different subtypes of VGLUT (VGLUT1, 2 and 3) have been identified. VGLUT1 and VGLUT2 are the dominant isoforms within central nervous system with high level of expression within hippocampus (Balschun et al., 2010). During early postnatal stages, VGLUT2 expression switches to VGLUT1 (Myazaki et al., 2003). Several neurological disorders including depression, Alzheimer's disease and Parkinson's disease have been linked to disruption of VGLUT1 and VGLUT2 (Moutsimilli et al., 2005; Kashani et al., 2006; Kirvell et al., 2006). Tordera et al. (2007) reported that mice with heterozygous knock down of VGLUT1 were impaired in long-term memory in the novel object recognition task. In another study,

deletion of VGLUT1 resulted in impaired hippocampal LTP in the CA1 region which was accompanied by a deficiency in spatial reversal learning (Balschun et al., 2010).

Glutamate receptors are divided into ionotropic and metabotropic receptors. Metabotropic receptors are indirectly gated G-protein coupled receptors, and ionotropic receptors are directly gated ion channels. Ionotropic receptors consist of N-methyl-D-aspartate (NMDA) and the α-amino-3-hydroxy-5-methyl-4-isoxazolepropionic acid (AMPA) receptor subtypes. NMDA receptors regulate the most common type of LTP in the CA1 region and dentate gyrus of the hippocampus (Harris et al., 1984; Malenka and Nicoll, 1993). Ca^{2+} entry through the NMDA receptor is essential for LTP. Downstream signaling effects of Ca^{2+} are believed to be mediated by the α-calcium-calmodulin-dependent proteinkinase II (CaMKII). While blocking the rise in postsynaptic Ca^{2+} prevents the induction of LTP, increasing the amount of postsynaptic Ca^{2+} by photolysis of caged Ca^{2+} can mimic LTP (Malenka et al., 1988). Research in behaving rats confirmed that hippocampal LTP at different synapses has different sensitivity to NMDA receptor antagonists (Leung and Shen, 1999). Non-NMDA dependent types of LTP have also been found at the mossy fiber to CA3, and Schaffer collaterals to CA1 (Zalutsky and Nicoll, 1990; Hanse and Gustafsson, 1994). This type of LTP may be mediated by voltage-gated Ca^{2+} channels (Johnston et al., 1992).

1.4 Subcortical inputs to the hippocampus

Neurons of the hippocampus receive inputs from many parts of the brain extrinsic to the hippocampus. Other than the entorhinal cortex, the major subcortical extrinsic

inputs to the hippocampus comes from the medial septum (MS) and vertical limb of the diagonal band of Broca (DBB).

1.4.1 Septohippocampal pathway

Medial septum and diagonal band of Broca (MS-DBB) are parts of the septal region that project to the hippocampus by four pathways: the fornix, the supracallosal striae, the fimbria, and the amygdalofugal route (Gaykema et al., 1990). Neurons located laterally in the medial septum project axons to the medial entorhinal cortex and ventral hippocampus (Gaykema et al., 1990). Lateral entorhinal cortex and dorsal hippocampus are innervated by neurons located in the medial portion of the MS and also by afferent inputs from caudal ventral limb of DBB and medial horizontal limb of DBB (Gaykema et al., 1990).

Immunohistochemical studies revealed three types of neurons projecting from MS-DBB to the hippocampus. These neurons were classified as both excitatory and inhibitory neurons. Cholinergic and glutamatergic neurons are excitatory while GABAergic neurons are inhibitory (Amaral and Kurz 1985; Manns et al., 2003; Sotty et al, 2003; Colom et al., 2005; Huh et al. 2010). Furthermore, firing patterns of MS-DBB neurons were classified based on characteristics such as the maximum firing frequency, duration of the after-hyperpolarizing potential, and the prominence of a hyperpolarization-activated current (Griffith et al., 1988; Serafin et al., 1996; Sotty et al., 2003).

Cholinergic MS-DBB neurons express choline acetyl transferase (ChAT) and are classified as slow-firing cells (Griffith & Matthews, 1986). Cholinergic neurons are

mostly located at the caudal and rostral portion of the MS-DBB. Septal cholinergic neurons innervate both GABAergic interneurons and the principal cells in the hippocampus (Leranth and Frotscher, 1987). On the other hand, septal GABAergic MS-DBB neurons, which express glutamic acid decarboxylase 67 (GAD67) and parvalbumin (Parv), target inhibitory hippocampal interneurons (Freund and Antal, 1988). Two firing patterns have been classified for the GABAergic neurons of the MS-DBB: i) fast-firing, ii) burst-firing (Morris et al., 1999; Knapp et al., 2000; Sotty et al., 2003). The highest density of GABAergic neurons is located on the middle portion of MS-DBB.

The third type of the MS-DBB neurons are glutamatergic neurons identified using vesicular glutamate transporter 2 (VGLUT2) (Sotty et al., 2003). These neurons constitute 4-23% of the projections from MS-DBB to the principal neurons of the CA1, CA3, and DG of the hippoampus and are distributed evenly within the MS-DBB (Colom et al., 2005, Huh et al., 2010). Glutamatergic neurons of MS-DBB fire in highly heterogeneous patterns including: slow-firing, fast-firing, burst-firing and cluster-firing which is unique to these neurons (Huh et al., 2010). Fast-firing glutamatergic MS-DBB neurons are the most abundant type with greatest concentration near the midline of the medial septum similar to the fast-firing GABAergic MS-DBB neurons (Huh et al., 2010). In addition to innervating the GABAergic and cholinergic neurons in the MS-DBB, septohippocampal glutamatergic neurons also innervate the inhibitory GABAergic interneurons and principal neurons in the hippocampus.

1.4.2 Brainstem to medial septum

Reticularis pontis oralis (RPO) and pedunclulopontine tegmental nucleus (PPT) are the two structures within the brainstem that provide ascending pathways to the medial septum (Macadar et al., 1974; Vertes, 1981; Vertes et al., 1993; Oddie et al., 1994). Neurons of the PPT innervate the supramammillary nucleus (SUM) and the septum while those ascending from RPO project to the posterior hypothalamic nucleus (PH). A series of experiments performed by microinfusion of cholinergic agonist carbachol into the PPT, PRO, SUM, and PH followed by recording LFP from the hippocampus revealed that majority of the ascending pathways originating from brainstem (PPT and RPO) and later from hypothalamic nuclei (SUM and PH) are cholinergic and are excitatory (Oddie et al., 1994). Neurons projecting from SUM to MS-DBB form synapses with both cholinergic and GABAergic neurons (Borhegyi et al., 1997). Furthermore, SUM also projects directly to the hippocampus innervating both principal cells (granule and pyramidal cells) and the GABAergic interneurons (Wyss et al., 1979; Haguland et al., 1984; Vertes, 1992; Nitsch and Leranth, 1996). In addition to the cholinergic projections a population of SUM neurons sends glutamatergic afferents to both MS-DBB and hippocampus (Kiss et al., 2000).

1.5 Hippocampal theta rhythm

The hippocampus produces a sinusoidal-like field potential that occurs at frequencies 4–10 Hz known as theta rhythm or rhythmical slow-wave activity (RSA). It has been shown that different neurotransmitters regulate the generation of hippocampal theta rhythm during different behaviors. Hippocampal theta rhythm is suggested to be

involved in attention, learning and memory formation, and the integration of motor programming.

1.5.1 Septal generation of the hippocampal theta rhythm

Medial septum and the vertical limb of the diagonal band of Broca (MS-DBB) are parts of the septal region that appear to be the most critical system for generating and maintaining the hippocampal theta oscillations in vivo. Lesion of the MS-DBB resulted in complete loss of the hippocampal theta rhythm in animals (Green and Arduini, 1954). Microinfusion of the cholinergic agonist carbachol into the medial septum of both anesthetized (Oddie et al., 1994) and freely behaving rats (Lawson and Bland, 1993) induced theta activity in the hippocampus. Intraseptal injection of muscimol, a GABA-A receptor agonist, abolished the theta rhythm (Oddie et al., 1996). However, intraseptal injection of 192 IgG-saporin a selective cholinergic neuron toxin in the septum, only decreased power of theta during walking, but failed to decrease the theta peak frequency in the behaving rats (Lee et al., 1994). Stimulation of septohippocampal cholinergic neurons of mice using optogenetics induced theta oscillations in urethane-anesthetized mice but not in walking mice (Vandecasteele et al., 2014). Optogenetic stimulation of septal cholinergic neurons significantly suppressed the power of LIA both during anesthesia and walking (Vandecasteele et al., 2014). Direct application of atropine to the MS eliminated the atropine-sensitive theta rhythm in the hippocampus in the rat under urethane anesthesia (Stewart and Fox, 1989). Medial septal injection of NMDA receptor antagonist decreased the amplitude of the hippocampal theta rhythm but not the frequency (Leung and Shen, 2004). This suppression of amplitude but not frequency was

similar to medial septal injection of the GABA-A receptor agonist muscimol (Bland et al., 1996). The frequency of theta has been suggested to come from the SUM in the hypothalamus (Kirk et al., 1998).

A model was proposed by Colom (2006) regarding the role of septohippocampal neurons in generation of the hippocampal theta rhythm. Based on this model, septo-hippocampal glutamatergic neurons get excited upon activation of septal cholinergic neurons. Excitation of gluamatergic neurons in conjunction with septal cholinergic cells provide the necessary excitatory background to initiate the theta frequency oscillations within hippocampus (Colom et al., 2006). At the same time, both septal cholinergic and glutamatergic neurons innervate the inhibitory GABAergic interneurons which allow the septal network to oscillate at theta frequencies (Colom et al., 2006). Rhythmic firing of the septohippocampal GABAergic neurons leads to rhythmic disinhibition of pyramidal cells of the hippocampus at the cell body region.

Multiple in-vitro studies have suggested that isolated hippocampus may show an intrinsic theta oscillation after cholinergic activation (Konopacki et al. 1987). Administration of a glutamatergic receptor agonist (S)-3,5-dihyroxyphenylglycine (DHPG), to isolated hippocampal slices induced a high frequency (6-10 Hz) theta rhythm (Gillies et al., 2002). Intrinsic theta oscillations in single cells are called membrane potential oscillations (MPOs). Depolarization of single hippocampal neurons, in the absence of synaptic transmission, is sufficient to induce theta-frequency MPOs, suggesting that MPOs arise from intrinsic properties of membrane currents (Leung and Yim, 1991; Leung, 2012). Theta generation from hippocampus itself was also reported in whole hippocampus preparation in vitro (Goutagny et al., 2009).

1.5.2 Two types of hippocampal theta rhythm

Vanderwolf first discovered a strong correlation between the moment-to-moment behavior and hippocampal EEG in behaving rats (Vanderwolf, 1969). Voluntary movements such as walking, running, and jumping (also known as Type 1 Behavior) and rapid eye movement (REM) sleep are accompanied by generation of high-frequency (6-10 Hz) and high-amplitude theta oscillations (Vanderwolf, 1969; Vanderwolf, 1975; Leung et al., 1982; Oddie and Bland, 1998). Theta rhythm can also be recorded from animals under anesthesia during electrical stimulation of the brainstem or in response to sensory stimuli (Stumpf, 1965a; Green, 1964; Bland, 1986; Herreras et al., 1988).

Awake-immobility (also known as Type 2 behavior) with the head held up against gravity and eyes open is accompanied by generation of a different theta rhythm (Vanderwolf, 1975). Theta oscillations during this type of behavior have a lower frequency (4-6 Hz) and are lower amplitude as compared to those recorded during voluntary movement (Vanderwolf, 1975; Bland and Oddie, 2001). During more autonomic behaviors including licking, chewing, and shivering and also during immobility large amplitude irregular activity (LIA) can be recorded in the hippocampus (Vanderwolf, 1969; Leung et al., 1982; Bland, 1986). Non-REM sleep and anesthesia are associated with slow oscillations (Wolansky et al., 2006).

The theta rhythm during different behaviors shows different pharmacological properties, suggesting the participation of different neurotransmitters during different behaviors (Vanderwolf, 1988; Dudar et al., 1979; Leung et al., 1982; Sainsbury et al., 1987; Leung 1998; Tai et al., 2011). Administration of cholinergic antagonists abolishes

the theta rhythm during awake-immobility (also known as Type 2 behaviors). Type 2 behaviors are also referred to as atropine-sensitive (Vanderwolf, 1975; Bland and Oddie, 2001). Furthermore, injection of cholinesterase inhibitors such as eserine induces atropine-sensitive theta (Bland, 1986). In another study by Tai et al. (2011) a continuous atropine-sensitive hippocampal theta rhythm was induced by vestibular stimulation during rotation when rats were immobile. Injection of atropine abolished this rotation-induced theta further demonstrates the role of cholinergic neurons in generation of hippocampal theta rhythm during Type 2 behaviors (Tai et al., 2011).

Theta rhythm which occurs along with voluntary movements (also known as Type 1 behaviors) is atropine-resistant. Injection of cholinergic antagonist drugs such as atropine sulphate and scopolamine, even at high doses, fails to abolish the theta rhythm during Type 1 behaviors. However, it is known that ACh was released in higher level in the hippocampus during Type 1 than Type 2 behaviors (Dudar et al., 1979), and ACh had stronger effect on hippocampal electrophysiological responses during walking than immobility (Leung, 1998). Other than ACh, several neurotransmitters may participate in the generation of atropine-resistant theta. Vanderwolf (1988) inferred that serotonin (5-HT) mediates the atropine-resistant theta rhythm because the combination of centrally acting atropine and 5-HT depletion in the hippocampus abolished the theta rhythm during Type 1 behaviors. 5-HT depletion was done by various means, including chemical depletion, selective lesion of median raphe neurons, sectioning of presumed 5-HT pathway to the hippocampus (Vanderwolf, 1988). Glutamate NMDA receptors in the septum and hippocampus may also be part of the atropine-resistant theta (Buzsaki, 2002; Leung and Desborough, 1988). NMDA receptor antagonist 2-amino-5-phosphonovaleric

acid administered in the medial septum or intracerebroventricularly attenuated the atropine-resistant theta in behaving rats (Leung and Desborough, 1988; Leung and Shen, 2004). Burst firing of the septohippocampal GABAergic neurons driving inhibitory hippocampal interneurons (Stewart and Fox, 1990) may be yet another component of the atropine-resistant theta rhythm. Septohippocampal GABAergic neurons are suggested to be critical for pacing hippocampal theta (Simon et al., 2006; Hangya et al., 2009).

Creation of these two genetically modified lines of mice was another approach to further prove that two types of theta oscillations co-exist. Shin et al. (2005) provided data showing that mice lacking phospholipase C (PLC)-ß1 lack one subset of the hippocampal theta rhythm. (PLC)-ß1 is one of the four PLC- ß isoenzymes that is highly expressed in the hippocampus within the septohippocampal pathway. Furthermore, PLC- ß1 is coupled to both muscarinic cholinergic receptors and to group I mGluRs in the hippocampus (Bland, 1986; Vertes and Kocsis, 1997; Stewart and Fox, 1990; Chuang et al., 2001). PLC-ß1$^{-/-}$ mice lacked the atropine-sensitive subtype of hippocampal theta rhythm observed during Type 2 behaviors while the atropine-resistant theta rhythm during Type 1 behaviors was intact (Shin et al., 2005).

1.5.3 Functions of the hippocampal theta rhythm

Synaptic plasticity within the hippocampus can be induced readily by burst stimulation at a theta frequency (Larson et al., 1986). Other studies showed that induction of LTP or LTD in the hippocampus depends on the phase of the theta during which stimulation was applied. Tetanic burst stimulation delivered on the peak of the theta rhythm recorded during Type 1 behavior induced LTP in stratum radiatum of CA1 region

of hippocampus; however, stimulation at the trough of the theta induced LTD (Hyman et al., 2003). The theta rhythm is believed to be important in spatial memory (Winson, 1978). After electrolytic lesion of the medial septum, rats were without a theta rhythm, and no longer able to perform the spatial tasks (Winson, 1978).

The hippocampal theta rhythm has a critical role in integration of sensory information and the neuronal processing required for the initiation of voluntary movements. Vanderwolf (1969) proposed that sensory processing in the hippocampus is accompanied by generation of the atropine-sensitive theta. Once a voluntary movement initiates, atropine-sensitive theta co-occurs with the atropine-resistant theta (Bland and Oddie, 1998). On the other hand, atropine-resistant theta rhythm is an indicator of the level of activation of motor systems engaged in voluntary movement (Vanderwolf, 1969). During Type 1 behaviors, frequency of the theta rhythm is linearly related to the speed of the movement while the amplitude of theta is linearly related with the magnitude of the movement (Vanderwolf, 1969). In an experiment performed by Bland et al. (2006), rats were trained to jump to the ledge (height adjustable) of a box in order to avoid shock. Rats produced atropine-sensitive theta just prior to jump avoidance response. Theta frequency increased as the height increased while amplitude of theta decreased (Bland et al. 2006).

1.6 Hippocampal gamma rhythm

Another type of oscillations that can be recorded from the hippocampus is the relatively high frequency gamma oscillations (30-150 Hz). Hippocampal gamma and theta rhythms appear to be independently generated (Leung et al., 1982; Leung 1992). In

the absence of theta rhythm, the power and regularity of gamma oscillation decrease and a slow irregular pattern of activity appears (Vanderwolf, 1969; Leung et al., 1982). Entorhinal cortex and the CA3 region of the hippocampus have been identified as the two independent generators of the hippocampal gamma rhythm (Bragin et al., 1995; Csicsvari et al., 2003; Colgin et al., 2009).

Using current source density (CSD) analysis, the largest estimated gamma-associated excitatory currents were found in the middle third of the dentate gyrus molecular layer (Bragin et al., 1995). Medial entorhinal cortex projections terminate in this zone of dentate gyrus (Bragin et al., 1995). Furthermore, lesions of the entorhinal cortex caused the gamma-associated excitatory currents to attenuate (Bragin et al., 1995). The gamma recorded in this region is coherent with excitatory currents recorded from stratum lacunosum layer of CA1 region which also receives inputs from entorhinal cortex (Charpak et el., 1995). In the study by Csicsvari et al. (2003), when the CA1 region of the hippocampus was set as the reference for detecting gamma, excitatory currents emerged from CA3. Although two gamma oscillators were reported to be usually independent, they can sometimes couple with each other (Colgin et al., 2009). It has been suggested that gamma oscillations generated via two different oscillators may produce different frequency bandwidths (Colgin et al., 2009). Low and high frequency gamma rhythms are correlated with CA3 and entorhinal cortex projections respectively. Low frequency gamma (~25-50 Hz) is most abundant during the descending part of the theta rhythm while high frequency gamma (~65-150 Hz) is maximal close to a theta rhythm trough (Bragin et al., 1995; Csicsvari et al., 2003; Colgin et al., 2009).

Many studies have supported the idea that gamma rhythm generation plays a role in both encoding and retrieval of memories. When human subjects were asked to remember lists of random words, intracranial recordings revealed an increase of gamma power during encoding the words that were subsequently recalled (Sederberg et al., 2007). In another study in behaving rats, it was concluded that high frequency gamma oscillations recorded from the CA1 region facilitated memory encoding since direct entorhinal cortex projections to CA1 convey information about the animal's current position in environment (Brun et al., 2008; Colgin et al., 2009). On the other hand, the amplitude of low frequency gamma oscillations originating from CA3 increased as animals learned to accurately perform a task that involved memory retrieval (Tort et al., 2009). Both memory retrieval and low frequency gamma rhythm are associated with increased gamma coherence between CA3 and CA1 while encoding memory and high frequency gamma are associated with increased gamma coherence between entorhinal cortex and CA1 region of hippocampus (Charpak et el., 1995; Montgomery and Buzsaki, 2007; Colgin et al. 2009).

1.7 Mice deficient for the vesicular acetylcholine transporter

Vesicular acetylcholine transporter (VAChT) is a twelve-transmembrane domain protein that stores ACh in synaptic vesicles by means of the electrochemical gradient produced by a V-type proton ATPase (Roghani et al., 1994). Proper storage of ACh in the synaptic vesicles via VAChT is necessary for efficient release of ACh from nerve endings (Parsons, 2000). A reduction of VAChT expression may result in a cholinergic deficit because of reduction of release of ACh into the synaptic cleft (Chen et al. 2011).

1.7.1 Heterozygous vesicular acetylcholine knock down mice

Prado et al. (2006) generated a line of genetically modified mice, named VAChT KD^{HET}, with selective knock down of VAChT gene. These mice were generated by targeting the 5' untranslated region of the VAChT gene by homologous recombination in a mixed 129S6/ SvEvTac (129S6) x C57BL/6J background and were backcrossed to C57BL/6/Uni for three generations (Prado et al., 2006). Due to altered expression of VAChT mRNA, these mice had 45% less VAChT protein within their central nervous system. Despite enhanced intracellular content of ACh (measured by high-performance liquid chromatography), release of ACh was reduced to almost 33%. Previous studies revealed that both muscarinic and nicotininc receptors played a role in social memory in mice (Kampen et al., 2004; Prediger et al, 2006). Consistent with these studies, VAChT KD^{HET} mice had a significant deficit in social recognition and were clearly impaired in remembering intruder mice when compared to wild-type mice (Prado et al., 2006). Similar to certain mouse models of AD (Dewachter et al., 2002) that had object recognition alterations, VAChT KD^{HET} mice performed worse in object recognition tests as compared to the wild-type mice (Prado et al., 2006). In another experiment by de Castro et al. (2009), VAChT KD^{HET} mice were injected with the cholinesterase inhibitor galantamine in order to clarify whether decreased VAChT levels affect encoding or retrieval of object recognition memory. Results indicated that increase of the cholinergic tone facilitated encoding information more effectively (de Castro et al., 2009).

1.7.2 Selective basal forebrain VAChT knock out mice

Martin-Silva et al. (2011) introduced a novel genetically modified mouse named $VAChT^{FloxNeo/FloxNeo}$ (Fig 1B). In order to generate these mice, one LoxP sequence was placed 260 bp upstream of the VAChT translational initiation codon. A second LoxP was added approximately 1.5kp downstream from the stop codon immediately followed by the Neomicin-resistance gene (TK-Neo cassette) which was followed by a third LoxP (Martin-Silva et al., 2011; Fig 1B). The embryonic stem cells were injected into C57BL/6J blastocytes to achieve the germ line transmission (Martin-Silva et al., 2011). Chimeric mice were bred with C57BL/6J mice and heterozygous mice generated (Martin-Silva et al., 2011). Finally, $VAChT^{FloxNeo/WT}$ mice were intercrossed and homozygous $VAChT^{FloxNeo/FloxNeo}$ mice were generated (Martin-Silva et al., 2011; Fig 1B). $VAChT^{FloxNeo/FloxNeo}$ had a 75% reduction of VAChT mRNA expression in brain. An increase of 1.4 fold in locomotion in open field was found in $VAChT^{FloxNeo/FloxNeo}$ mice as compared to wild-type mice (Martin-Silva et al., 2011). The Neo cassette was removed from $VAChT^{FloxNeo/FloxNeo}$ mice and $VAChT^{Flox/Flox}$ mice was generated.

The Nkx2.1Cre mice were generated in the C57/BL6 strain by pronuclear injection of linearized bacterial artificial chromosome (BAC) in which fifteen base pairs at the 5□ of exon 2 were replaced with Cre-polyA (Xu et al. 2008; Fig 1A). These mice were previously used to remove choline acetyltransferase from the forebrain (Patel et al., 2012). The Nkx2.1Cre mice were crossed with $VAChT^{Flox/Flox}$ mice and $VAChT^{Nkx2.1\text{-}Cre\text{-}flox/flox}$ mice were generated which have a selective knock out of VAChT specific to basal

forebrain including the septohippocampal cholinergic neurons (Al-Onaizi et al., under review).

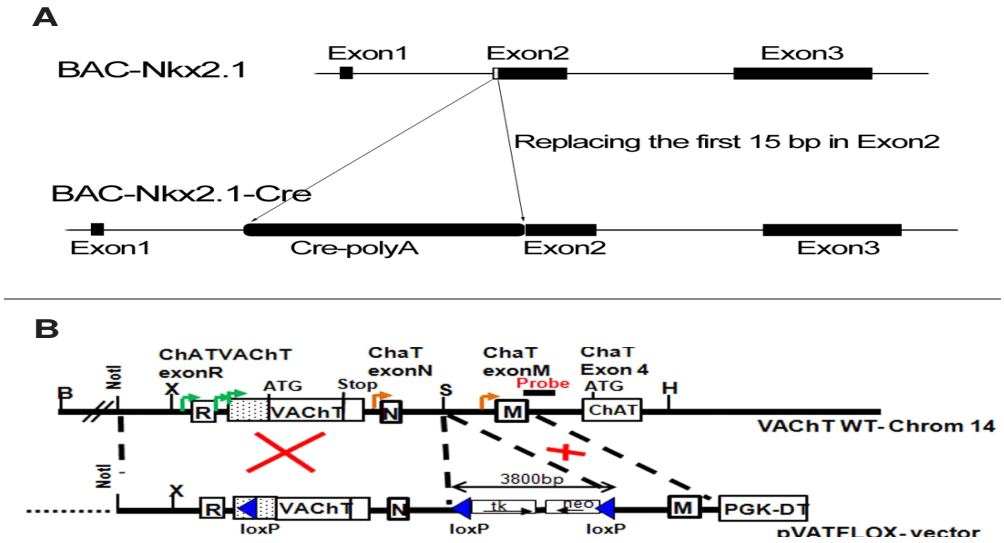

Figure 1 Schematic drawing of generation of Nkx2.1Cre and VAChT$^{FloxNeo/FloxNeo}$ mice. **A)** Fifteen base pairs at the 5' of exon 2, including the ATG, were replaced with Cre-polyA (Xu et al., 2008). **B)** Boxes represent the different exons of ChAT or VAChT. The position of the initiation codon (ATG) for VAChT and ChAT and the stop codon (Stop) of VAChT are indicated. Potential transcription initiation sites are indicated for VAChT (green arrowheads) and ChAT (orange arrowheads). Note that the VAChT gene is within the first intron of ChAT (Martin-Silva et al. 2011).

1.8 Rationale and hypothesis

In rodents, activation of the hippocampus is manifested by increase in theta (4-10 Hz) and gamma (30-100 Hz) oscillations in the electroencephalogram (EEG). Acetylcholine (ACh) has a critical role in cortical activation and modulation of cognitive function and synaptic plasticity (Rasmusson, 2000). The hippocampal theta rhythm during awake-immobility consists of a cholinergic component (Vanderwolf, 1988;

Leung, 1998). Disruption of the central ACh function is an early pathology of Alzheimer's disease (Francis et al., 1999; Coben, 1985). Mice with heterozygous knock down of the VAChT gene (VAChT KD^{HET}) showed reduction in release of ACh from central cholinergic nerve terminals of ~ 33% (Prado et al., 2006). Mice with forebrain knockout of the VAChT gene (Martyn et al., 2012) had negligible ACh release within their forebrain. While multiple behavioral deficits were observed in these genetically modified mice with reduced levels of VAChT, the electrophysiological substrate for these changes has not been studied. Therefore, whether hippocampal activation is affected in these two mutant mouse lines is unknown.

We first aimed to record local field potentials (LFPs) from CA1 region (stratum radiatum) of hippocampus of these two genetically modified lines of mice during walking and awake-immobility. Their wild-type littermates were used as control. We hypothesized that mutant mice will manifest hippocampal theta and gamma rhythms different from control mice. Second, we explored the effect of administration of a muscarinic cholinergic antagonist drug on hippocampal activation of such genetically modified mice during different behaviors. We hypothesized that sensitivity of hippocampal activation of both lines of genetically modified mice to the drug will be similar to the control mice as their deficiency is in expression of VAChT and not the muscarinic receptor. Finally, we investigated the role of glutamatergic neurons in generation of theta and gamma rhythms during different behaviors in these genetically modified mice by injecting the NMDA receptor antagonist 3-[(R)-2-carboxypiperazin-4-yl]-prop-2-enyl-1-phosphonic acid (CPP). We hypothesized that administration of CPP will cause abnormal hippocampal activation of all mice especially during walking.

2 Material and methods

2.1 Mutant and control mice

The experiments were performed on two groups of genetically modified. The first group of mutant mice, named VAChT KD^{HET}, had a heterozygous knock-down of the vesicular acetylcholine transporter (VAChT) in the brain (Prado et al., 2006). VAChT is responsible for packaging and release of acetylcholine from synapses. Heterozygous mutant VAChT mice (VAChT KD^{HET}) were backcrossed with C57BL/6J animals for three generations (Prado et al. 2006). Three of their wild-type littermates were used as control mice.

The second group of mice, named $VAChT^{Nkx2.1\text{-}Cre\text{-}flox/flox(+,+)}$, had VAChT deletion restricted to the forebrain, by crossing Nkx2.1-Cre mouse line (C57BL/6J-Tg(Nkx2-1- cre)2Sand/J), with $VAChT^{flox/flox}$ mice (crossed for 5 generations with C57BL/6J) (Al-Onaizi et al., under review). Three of the $VAChT^{Nkx2.1\text{-}Cre\text{-}flox/flox(+,+)}$ mice littermates were used as control mice. These control mice had the LoxP however expression of VAChT was not affected and they were named $VAChT^{Nkx2.1\text{-}Cre\text{-}flox/flox(-,-)}$.

Hereafter, control mice including both wild-type and $VAChT^{Nkx2.1\text{-}Cre\text{-}flox/flox(-,-)}$ mice will be referred to as WT (Wild-Type) mice, VAChT KD^{HET} will be referred to as HET (Heterozygous) mice and $VAChT^{Nkx2.1\text{-}Cre\text{-}flox/flox(+,+)}$ mice will be referred to as KO (Knock Out) mice. Mice were housed in groups of 3 to 4 in each cage, with food and water available ad libitum. Temperature of the room was maintained at 22°C ± 1 with with a 12/12 h light/dark cycle beginning at 7 a.m. All surgical and experimental

procedures were approved by the Animal Use Subcommittee of the University of Western Ontario Council on Animal Care, in accordance with Canadian Council of Animal Care policy.

2.2 Electrode implantation

The experiments were conducted on 18 adult male mice 6 HET mice, 6 KO mice, and 6 WT mice (3 of which were littermates of HET mice and the other 3 littermates of KO mice) weighing 28-54 g. Animals were anesthetized with ketamine (100 mg/kg) and xylazine (25 mg/kg) in 0.9% saline (intraperitoneal, i.p.). During the surgery, anesthetic condition of the animal was tested every 20 minutes by toe pinching and a supplementary dose was injected if needed. The head of the animal was fixed on to a stereotaxic frame using blunt ear bars and the skull was adjusted to fit the lambda and bregma in the same horizontal plane. Throughout the implantation, body temperature was maintained between 35-37°C using a rectal thermometer. The skull was exposed and two small holes were drilled bilaterally over the hippocampal CA1 region (AP -2.3 mm, L ± 1.6 mm) based on the coordinates of the mouse brain atlas (Franklin and Paxinos 1998). An electrode comprised of a 125-μm Teflon-insulated stainless steel wire recording from one cut end, and soldered to a female miniature connector at the other end. Two electrodes were bundled together for placement in the CA1 region of the hippocampus with the deep electrode targeting the stratum radiatum and the shallow one targeting the alveus. A small hole was drilled over the left cerebellum and another one drilled over the right frontal cortex. A jeweller's screw was placed over each of these holes and served as a recording ground. Next, a thin layer of cyanoacrylate (Krazy Glue) was applied over the skull.

Finally, electrodes and screws were fixed using dental cement. In order to avoid loss of the head cap, mice were housed individually in a large cage (25cm x 40cm x 15cm) after the implantation.

2.3 Recording and analysis

The mice were allowed 4-6 days to recover from surgery. Later, a cable was connected to the electrodes via the female miniature connector pins on the head cap. A mouse was placed in a cubic plastic cage (30 cm x 30 cm x 30 cm) and allowed to habituate for 10 minutes to the recording environment. Hippocampal LFP was recorded from the freely behaving mouse during periods of awake-immobility and walking. The behavior of the mouse was visually monitored and annotated during the recording of LFP. A mouse was considered to be awake-immobile when it was motionless in an alert state with its head held up against gravity and eyes open. Ear flicks, eye blinks and movement of nostril during immobility were also included as part of the awake-immobility behavior. Besides the regular walking, other behaviors including running, rearing, turning, digging and postural movements were also considered as walking behavior. Hippocampal LFP was recorded for 30-45 minutes (each record was 60 seconds long) from the mouse as a baseline condition. Then, 5 mg/kg i.p. scopolamine hydrochloride (muscarinic cholinergic antagonist) was injected (i.p.), and LFP recordings stated 10 minutes after injection for another 30-45 minutes. A week after the first recording, mice were experimented again under the same procedure however during the second recording instead of scopolamine a 10 mg/kg i.p. dose of NMDA receptor

antagonist CPP (3-[(R)-2-carboxypiperazin-4-yl]-prop-2-enyl-1-phosphonic acid) was injected.

The power spectrum was constructed from averaging at least 15 segments LFP of each behavior (awake-immobility or walking), either for baseline or after injection of a drug. Segments of the LFP recordings were selected manually in order to eliminate any artifacts. Each segment was 1024 points or 5.12 s with 200 Hz sampling (Leung et al., 1982). Six average power spectra were plotted for each mouse, for the following condition: i) awake-immobility, ii) scopolamine awake-immobility, iii) CPP awake-immobility, iv) baseline walking, v) scopolamine walking and vi) CPP walking. Each spectrum had a frequency resolution of 0.19 Hz (1/5.12 s), and elliptical smoothing over 5 bins made statistically independent values were separated by 5 bins, or 0.95 Hz, but with more than 150 degrees of freedom. Power spectra were plotted in arbitrary logarithmic units, with the calibration of 5.43 log units = 1 mV peak-to-peak amplitude of a sine wave. An increase of 1 logarithmic power unit signified a 10-fold increase in the squared amplitude of the LFP at a specific frequency.

2.4 Histology

At the end of experiments, mice were deeply anesthetized with 30% urethane and perfused through the heart with 100 ml of cold saline followed by 100 ml of cold 4% formaldehyde. The brain was extracted from the cranium and placed in 4% formaldehyde solution until ready for sectioning. Coronal brain sections of 40 µm thick were cut using a freezing microtome and mounted on slides and stained with thionin. Electrode

placements were verified by 100X magnification of the slides using a microscope. Photos were taken from brain sections using a digital camera.

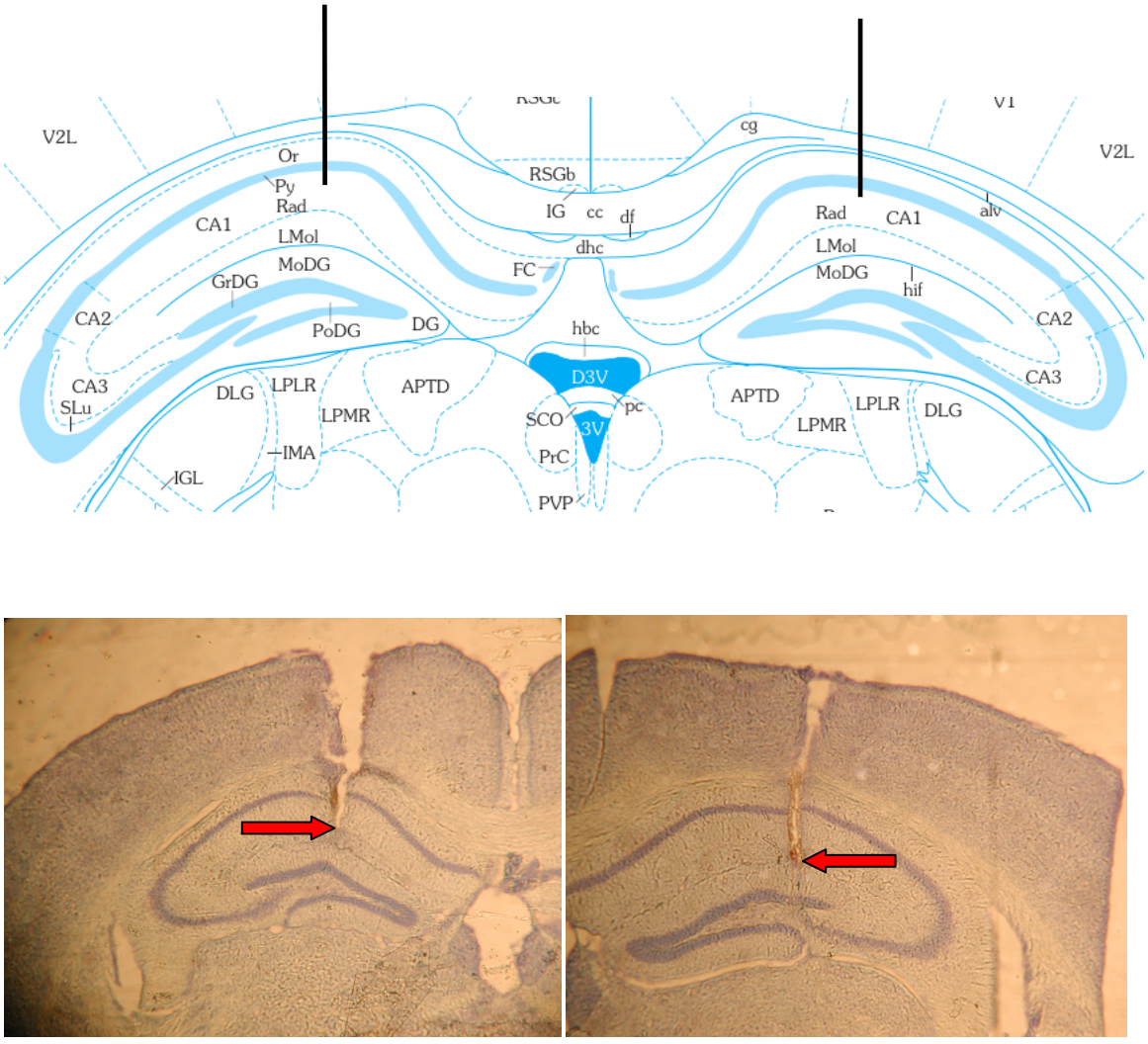

Figure 2 Top: Hippocampal CA1 region (AP -2.3 mm, L ± 1.6 mm) based on the coordinates of the mouse brain atlas (Franklin and Paxinos 1998) Bottom: Coronal brain sections (left and right side) stained with thionin. Electrode placements (red arrows) were verified by magnification of the slides using a microscope.

2.5 Statistical analysis

Four measures were obtained from each power spectrum derived from a single mouse: i) theta peak frequency (3-10 Hz), ii) theta peak rise (logarithmic units), iii) average logarithmic power of low gamma frequency (30-58 Hz) and iv) average logarithmic power of the high gamma frequency (62-100 Hz). The theta peak rise is the difference between the power (in logarithmic units) at the theta peak (maximum) and the power of the valley (minimum) immediately before the theta peak. Theta peak rise gives an indication of the power of the rhythmic oscillations at the theta frequency. All data were expressed as mean ± standard error of the mean (SEM) when applicable. All statistics were performed using the GraphPad Prism 5.0 software. Each of the 4 variables introduced above was subjected to several two-way Analysis of Variance (ANOVA) or paired t-tests. The groups of mice (WT, HET and KO) was set as a between factor and behavior (walking/awake-immobility) was set as a within factor. In some of the two-way ANOVAs performed, effect of the drug (scopolamine hydrochloride/CPP) on any of the above variables was set as the within factor rather than the behavior. Statistical significance was set at $P < 0.05$.

3 Results

3.1 Baseline LFP recording during awake-immobility and walking

Local field potentials (LFPs) were recorded from CA1 region of hippocampus of 18 adult male mice (6 Wild-Type mice (WT), 6 VAChT KD^{HET} mice (HET), and 6 $VAChT^{Nkx2.1\text{-}Cre\text{-}flox/flox}$ mice (KO)). Mice were placed in a cubic cage (30 cm x 30 cm x 30 cm) and allowed ten minutes to habituate. LFPs were recorded for 30-45 minutes while mice were freely behaving. Three of the control mice were wild-type littermates of the HET mice and the other three were $VAChT^{Nkx2.1\text{-}Cre\text{-}flox/flox(-,-)}$ mice. No significant difference was seen in case of any of the experimental results (theta peak frequency and power, low- and high-frequency gamma power, and response to drugs) between these two control groups (paired t-tests and 2-way ANOVAs, n = 3, $P > 0.05$) thus we considered them all as WT mice.

During awake-immobility, the frequency of theta rhythm was stable at ~ 5 Hz as indicated by time-frequency spectrogram (Fig. 3B) and the LFPs (Fig. 3C). During awake-immobility, the average theta rhythm peak frequency recorded from 6 WT mice was 4.47 ± 0.21 Hz (Fig. 6-7), with a rise of theta peak of 0.53 ± 0.03 log unit (Fig. 6-7). Theta peak frequency increased to about 8 Hz during walking, as shown by the LFPs and spectrogram of a representative mouse (Fig. 3B, C). As a group, theta frequency in WT mice was higher during walking as compared to awake-immobility (7.77 ± 0.15 Hz, n = 6, paired t-test, $P < 0.001$; Fig. 7). WT mice manifested significantly higher theta power

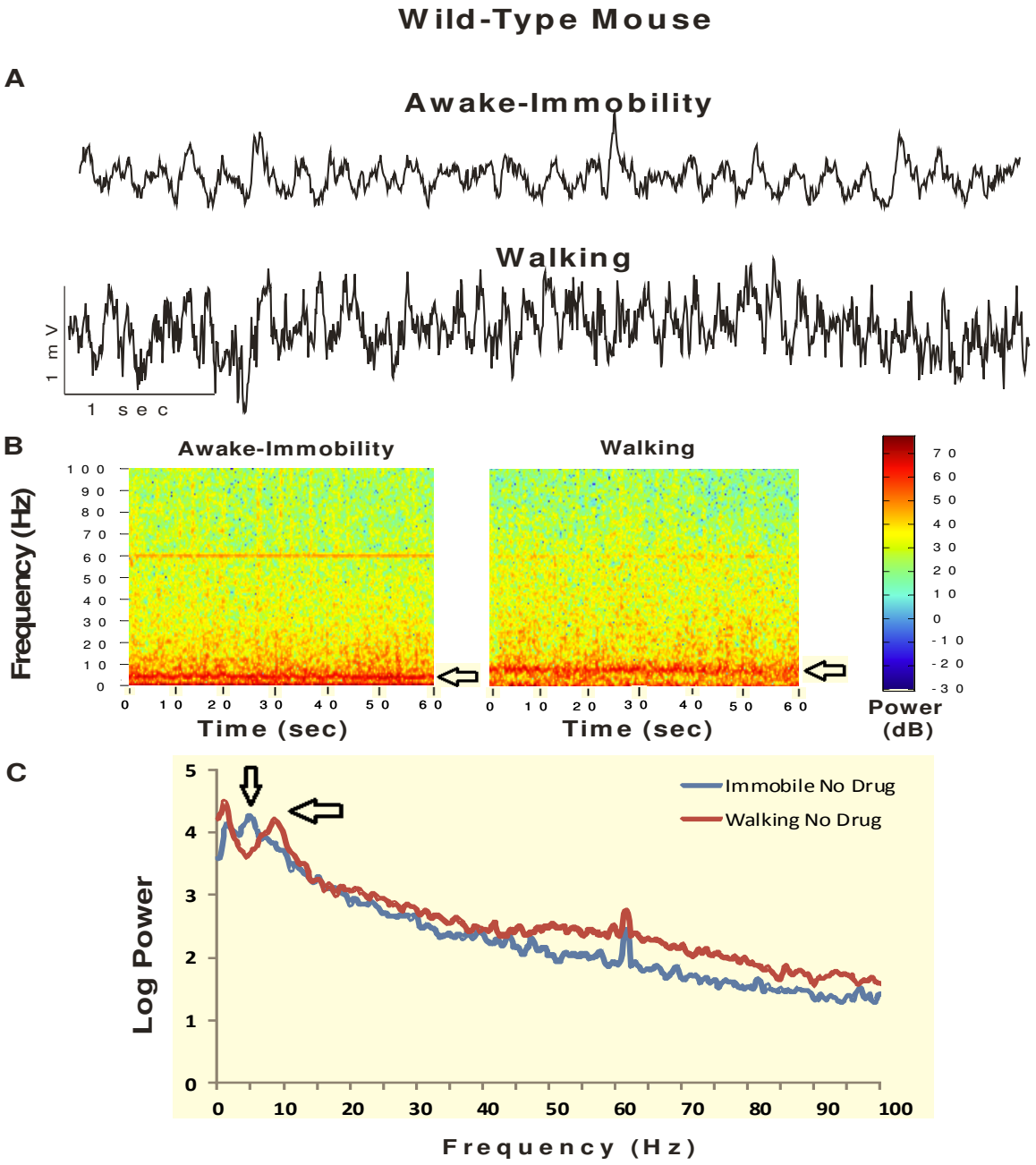

Figure 3 Hippocampal activation of a representative wild-type (WT) mouse. **A)** Representative LFP traces recorded from CA1 stratum radiatum of a WT mouse during awake-immobility (top) and walking (bottom). **B)** Time-frequency spectrogram indicates relatively stable theta frequency during 60 sec of recording (horizontal axis); the vertical axis represents frequency from 0 to 100 Hz, with color (red: strong, blue: weak) intensity calibration in power (dB). 20 dB is equal to 1 log power unit. **C)** Power spectra of hippocampal LFPs during awake-immobility (blue trace) and walking (red trace). Theta rhythm during awake-immobility was lower in frequency and amplitude as compared to the same measure recorded during walking. Gamma power at 50-100 Hz was higher during walking than awake-immobility.

during walking as compared to awake-immobility (0.86 ± 0.07 log units, n = 6, paired t-test, $P < 0.001$; Fig. 7). Low-frequency (30-58 Hz) gamma power did not change significantly with behavior (awake-immobility: 2.40 ± 0.09 log units, walking: 2.55 ± 0.09 log units, n = 6), as confirmed by paired t-test $P > 0.05$; Fig. 7). However, high-frequency (62-100 Hz) gamma power was significantly larger during walking as compared to awake-immobility (awake-immobility: 1.85 ± 0.09 log units, walking: 2.12 ± 0.12 log units, n = 6), as shown by paired t-test $P < 0.001$; Fig. 7).

Theta peak frequency of HET mice during awake-immobility and walking was 4.92 ± 0.03 Hz and 8.34 ± 0.15 Hz, respectively (n = 6; Fig. 6-7). HET mice showed a significantly higher theta power during walking (0.89 ± 0.04 log units) as compared to awake-immobility (0.40 ± 0.02 log units, n = 6, paired t-test, $P < 0.0001$; Fig. 6). Both low- and high- frequency gamma power were significantly stronger during walking as compared to awake-immobility (n = 6, paired t-test, $P < 0.01$; Fig. 6). The average logarithmic power of low-frequency gamma oscillations of 6 HET mice was 2.60 ± 0.15 log units during awake-immobility and 2.79 ± 0.08 log units during walking (Fig. 6).

Higher theta frequencies were found in HET mice as compared to WT mice at a fixed behavior (Fig. 7); the difference was statistically significant during walking (2-way ANOVA group effect, $F_{(1, 10)} = 12.87$, $P < 0.05$) but not during awake-immobility. During awake-immobility, the theta power in HET mice was lower than that in WT mice (2-way ANOVA group effect $F_{(1, 10)} = 60.29$, $P < 0.05$; Fig. 7). Results of a 2-way ANOVA (group x behavior) revealed that between WT and HET mice, there was no significant difference in the power of low-frequency gamma rhythm during either of the behaviors ($F_{(1, 10)} = 0.07$, $P = 0.80$; Fig. 7). Similar results were obtained for high

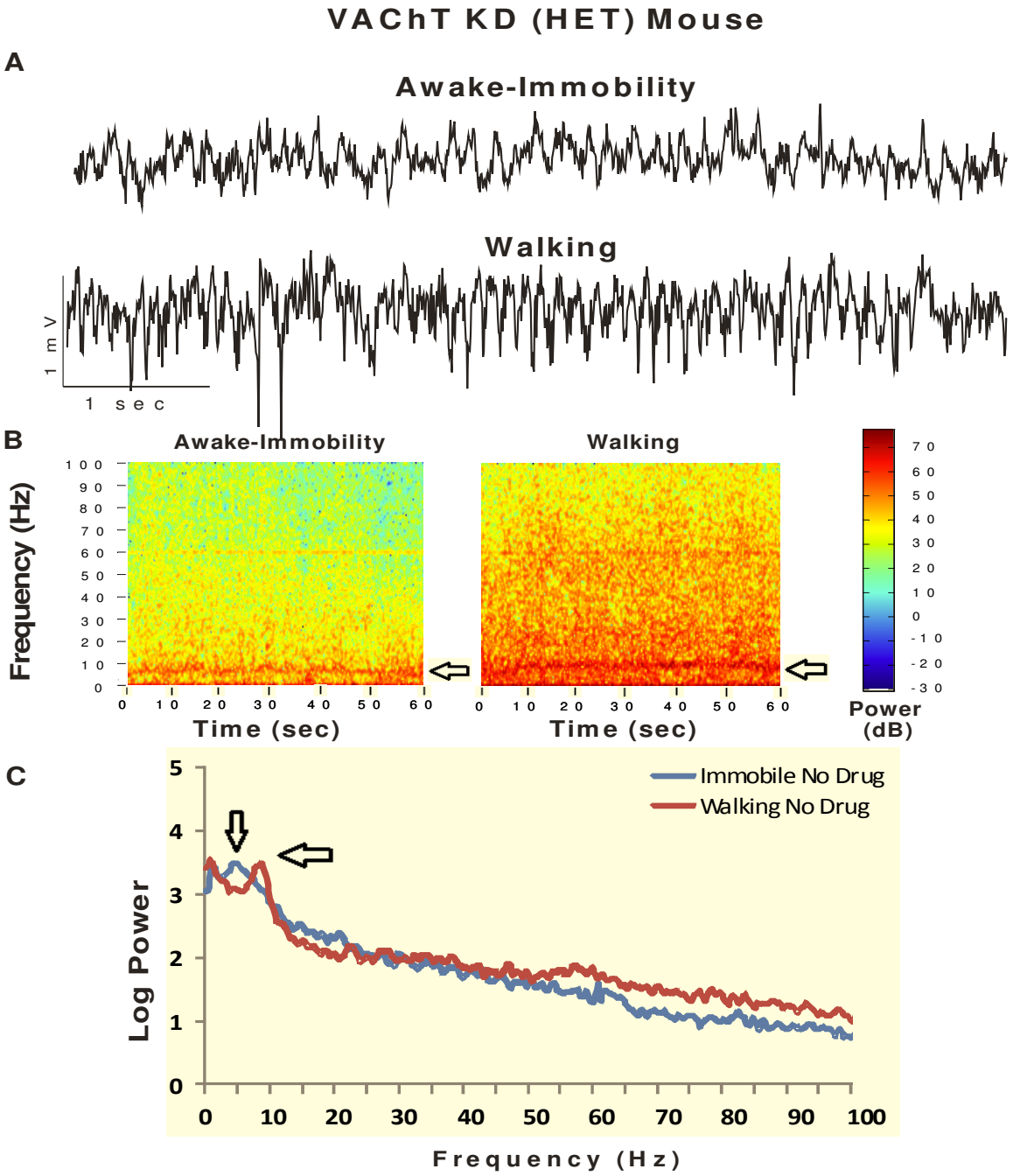

Figure 4 Hippocamapal activation of a representative VAChT KD^{HET} mouse. **A)** LFP traces recorded from the CA1 region of the hippocampus of a HET mouse during awake-immobility (top) and walking (bottom). **B)** Time-frequency spectrogram indicates stable theta frequency during 60 sec of recording, and the higher gamma power during walking than immobility. **C)** Power spectra during awake-immobility (blue trace) and walking (red trace). Theta rhythm during awake-immobility was lower in frequency and amplitude as compared to the same measure recorded during walking. Power of gamma is significantly higher during walking.

frequency gamma oscillations (2-way ANOVA group effect, $F_{(1, 10)} = 0.01$, $P = 0.91$; Fig. 7).

Walking in KO mice was accompanied by significantly higher theta power (0.93 ± 0.03 log unit) and higher peak frequency theta rhythm (7.83 ± 0.20 Hz, n = 6, paired t-test, $P < 0.001$; Fig. 6) as compared to the same measure during awake-immobility (3.81 ± 0.19 Hz, 0.09 ± 0.02 log unit). Power of the low-frequency gamma in KO mice increased significantly during walking (2.86 ± 0.12 log units) as compared to awake-immobility (2.55 ± 0.13 log units, n = 6, paired t-test, $P < 0.001$; Fig. 6). Similar results were observed for high-frequency gamma power (awake-immobility: 1.76 ± 0.11 log units, walking: 2.07 ± 0.11 log unit, n = 6, paired t-test, $P < 0.05$; Fig. 6).

Compared with WT mice, KO mice manifested a significantly lower theta peak frequency during awake-immobility (2-way ANOVA group factor, $F_{(1, 10)} = 4.65$, $P < 0.05$; Fig. 7). Furthermore, awake-immobility theta showed significantly lower power in KO mice than in WT mice (2-way ANOVA group factor, $F_{(1, 10)} = 55.82$, $P < 0.001$; Fig. 7). No significant difference in theta peak frequency was observed between WT (7.77 ± 0.15 Hz) and KO mice (7.83 ± 0.20 Hz) during walking (2-way ANOVA group factor, $F_{(1, 10)} = 0.05$, $P = 0.83$; Fig. 7). Also, there was no significant difference in the walking theta power between WT (0.86 ± 0.07 log unit) and KO mice (0.93 ± 0.03 log unit) (2-way ANOVA group factor, $F_{(1, 10)} = 0.06$, $P = 0.82$; Fig. 7).

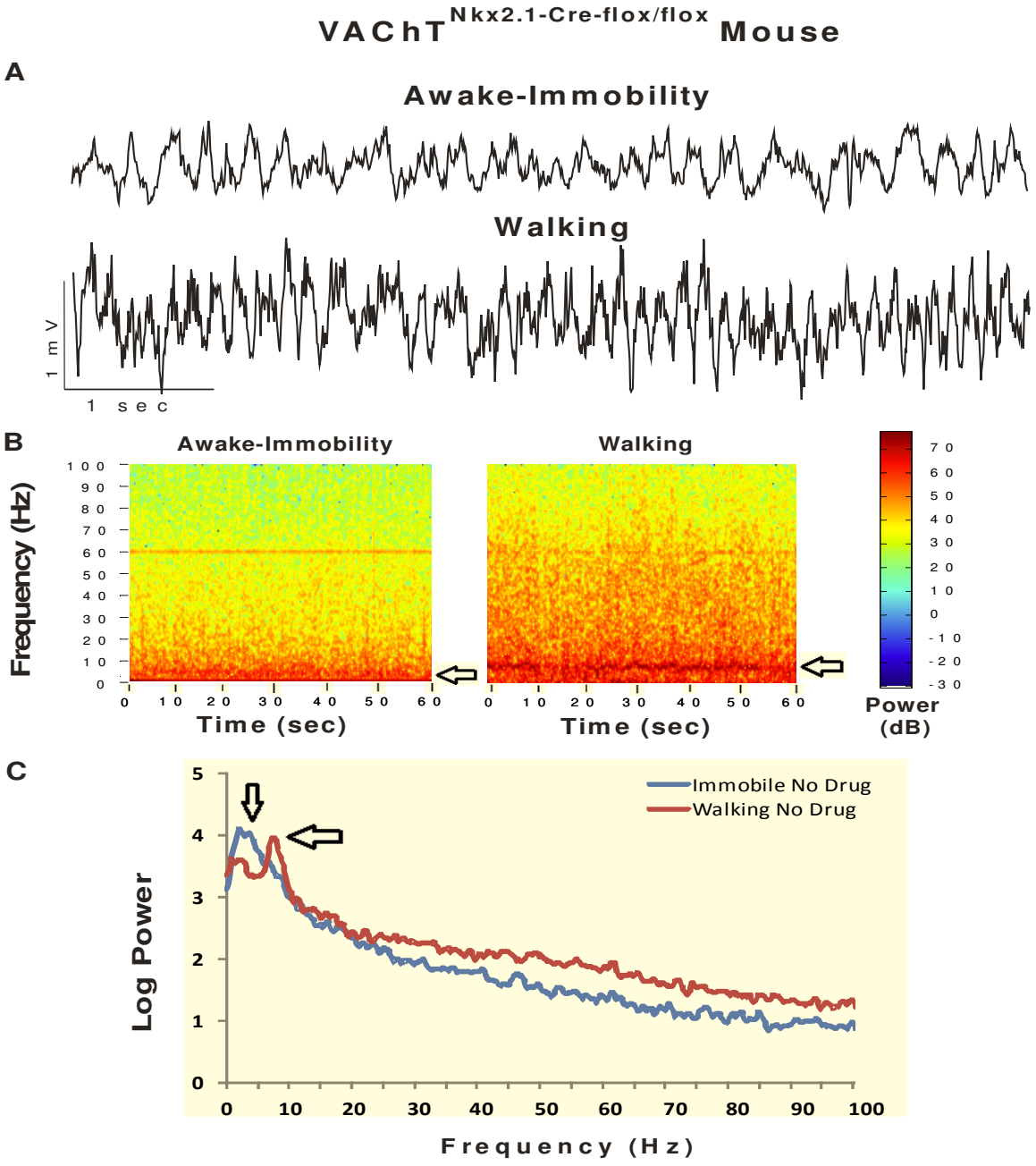

Figure 5 Hippocamapl activation of a representative VAChT$^{Nkx2.1\text{-}Cre\text{-}flox/flox}$ mouse. **A)** LFP traces recorded from the CA1 region of the hippocampus of a HET mouse during awake-immobility (top) and walking (bottom). **B)** Time-frequency spectrogram indicates stable theta frequency during 60 sec of recording, and the higher gamma power during walking than immobility **C)** Power spectra during awake-immobility (blue trace) and walking (red trace). Theta rhythm during awake-immobility was lower in frequency and amplitude as compared to the same measure recorded during walking. Power of gamma is significantly higher during walking.

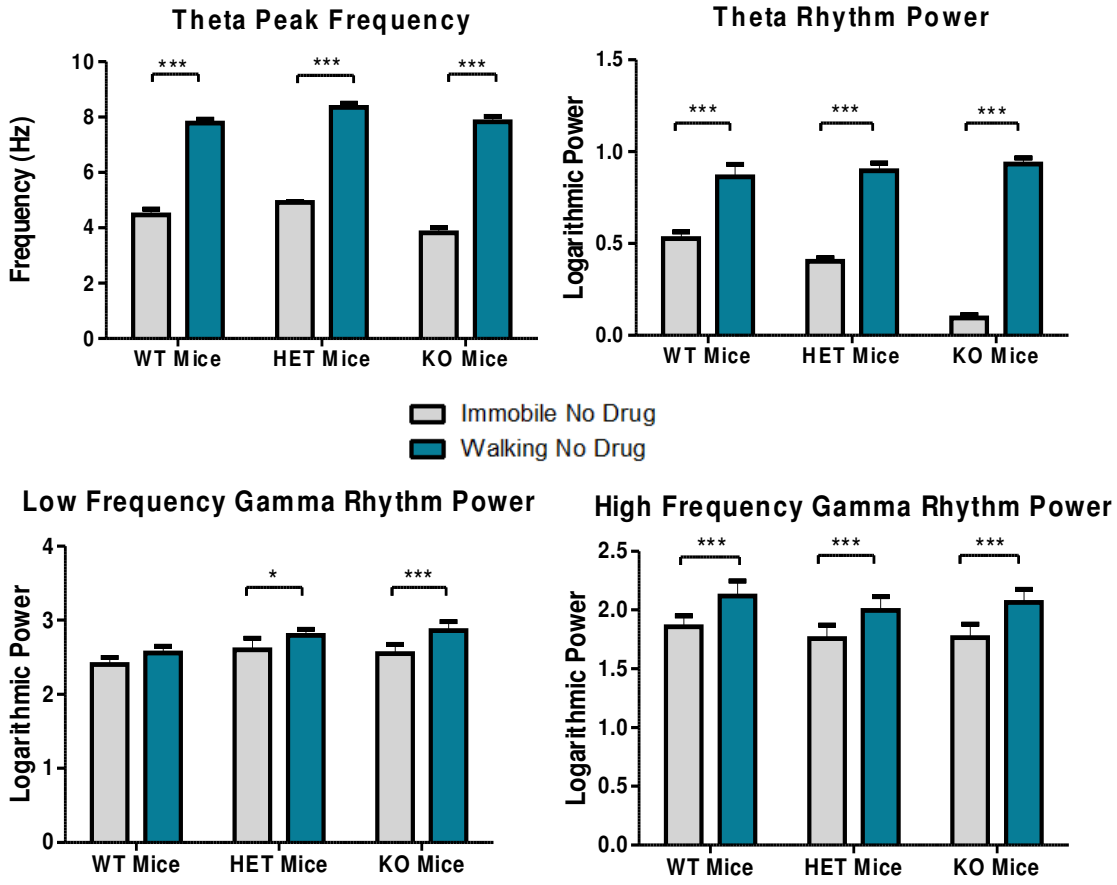

Figure 6 Effects of behavior on hippocampal activation of WT (n = 6), HET (n = 6), and KO (n = 6) mice. Values are expressed as mean ± SEM. * $P<0.05$, *** $P<0.001$: difference between awake-immobility and walking using repeated measures two-way ANOVA followed by Bonferroni test. *In each group of mice,* theta was higher in power and peak frequency, and high-frequency gamma was higher during walking as compared to the same measure during awake-immobility. In HET and KO mice, but not in WT mice, low-frequency gamma was higher during walking than immobility.

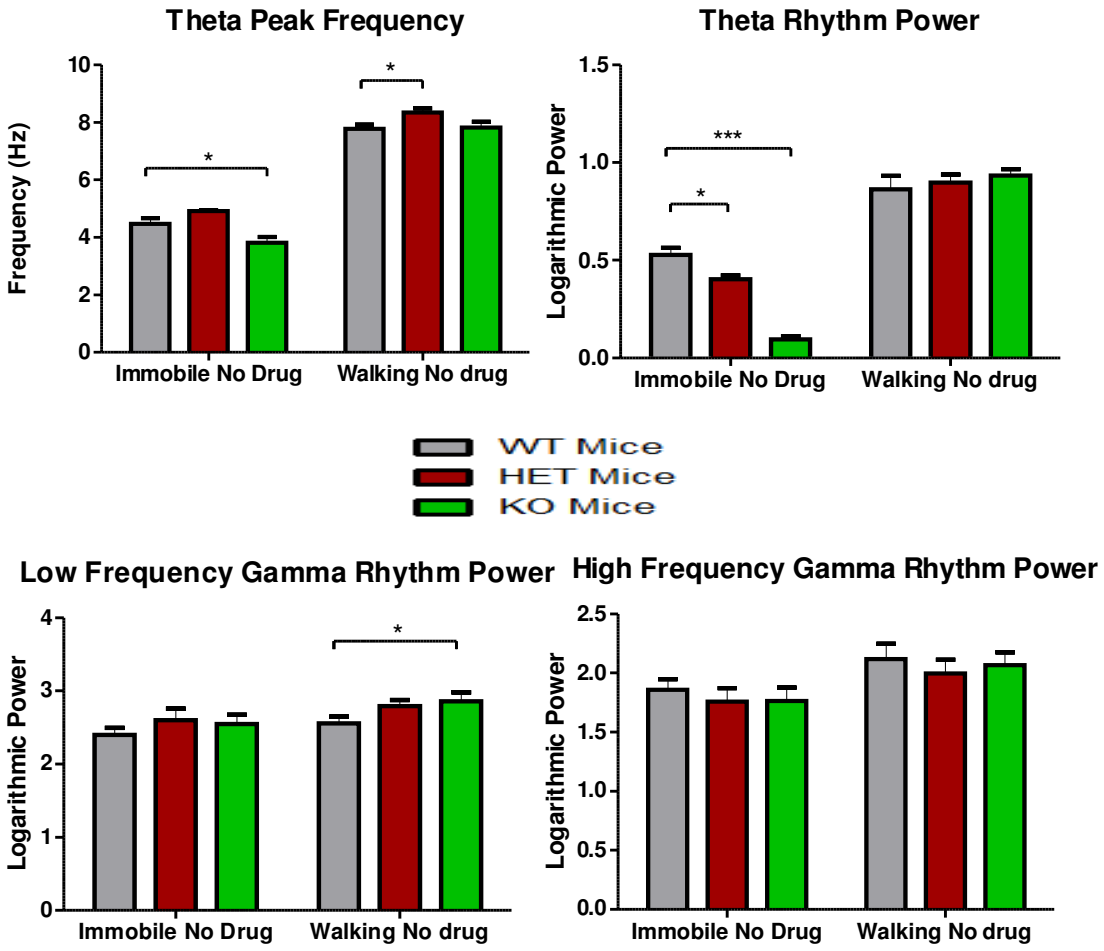

Figure 7 Comparison of hippocampal activation of WT (n = 6), HET (n = 6), and KO (n = 6) mice. Values are expressed as mean ± SEM. * $P<0.05$, *** $P<0.001$: difference between groups using repeated measures two-way ANOVA followed by Bonferroni test. *Awake-immobility*: Theta peak frequency is significantly higher in WT mice as compared to KO mice. Theta power decreases in the order of WT, HET and KO mice. No significant group differences were observed for the power of low- or high-frequency gamma rhythm. *Walking*: HET mice manifested significantly higher theta peak frequency as compared to WT mice. Theta power did not differ significantly amongst the groups. Low-frequency gamma power of KO mice during walking was significantly stronger than WT mice.

3.2 Injection of scopolamine hydrochloride

In order to evaluate the response of mutant mice to a cholinergic antagonist drug, mice from all groups were injected with the muscarinic cholinergic antagonist scopolamine hydrochloride (5 mg/kg i.p.). Ten minutes post injection, LFPs were recorded for another 30 to 45 minutes. Results obtained from both mutant groups were compared with the WT mice.

3.2.1 Wild-type mice

Scopolamine hydrochloride abolished the awake-immobility hippocampal theta rhythm in WT mice (Fig. 8, 14). By contrast, during walking, scopolamine injection resulted in a non-significant decrease of theta rhythm peak frequency (7.64 ± 0.32 Hz; n = 6; P = 0.72; paired t-test; Fig 9, 15). However, power of theta was suppressed significantly after injection of scopolamine (0.44 ± 0.04 log units; n = 6, $P < 0.001$; paired t-test; Fig. 9, 15). A two-factor ANOVA (behavior x drug) followed by Bonferroni test was performed to analyze the effects of scopolamine injection on hippocampal gamma oscillations. No significant change was observed in power of low frequency gamma after administration of scopolamine during both behaviors (n = 6, $F_{(1, 10)} = 1.77$, P = 0.21; Fig. 8-9, 14-15). Average logarithmic power of low gamma during awake-immobility and walking were 2.41 ± 0.11 and 2.62 ± 0.24 log units respectively (Fig. 14, 15). High frequency gamma power (awake-immobility: 1.87 ± 0. 14 log units, walking: 2.03 ± 0.16 log units) also did not change significantly after injection of scopolamine (2-way ANOVA, n = 6, $F_{(1, 10)} = 0.06$, P = 0.81; Fig 8-9, 14-15).

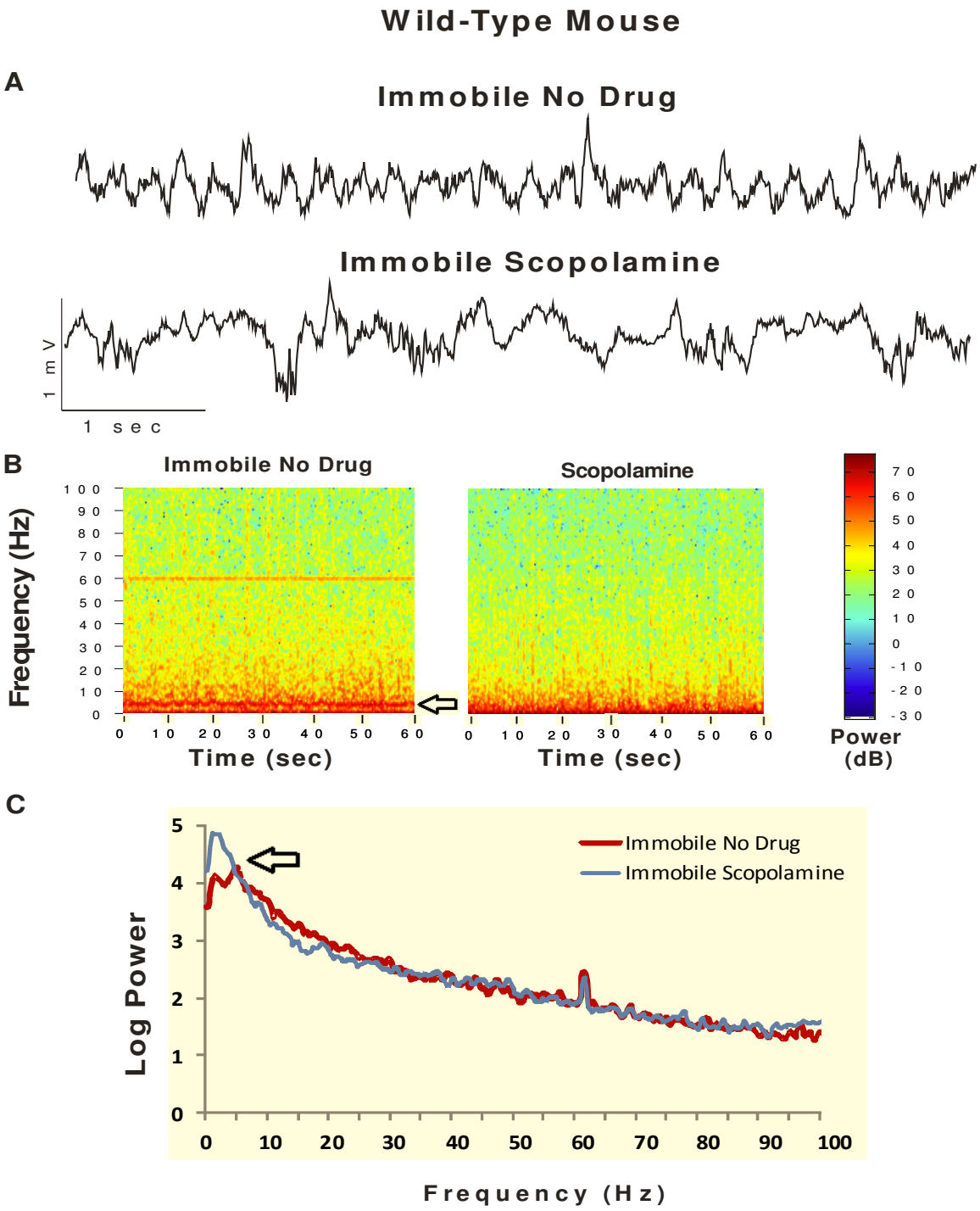

Figure 8 Effects of administration of scopolamine on hippocampal activation of a representative wild-type mouse during awake-immobility. **A)** LFP traces (6 seconds) before and after scopolamine injection. **B)** Time-frequency spectrogram and **C)** Power spectra before (red trace) and after administration of scopolamine (blue trace). Scopolamine injection abolished the theta peak during awake-immobility, but did not change significantly the low- and high-frequency gamma power.

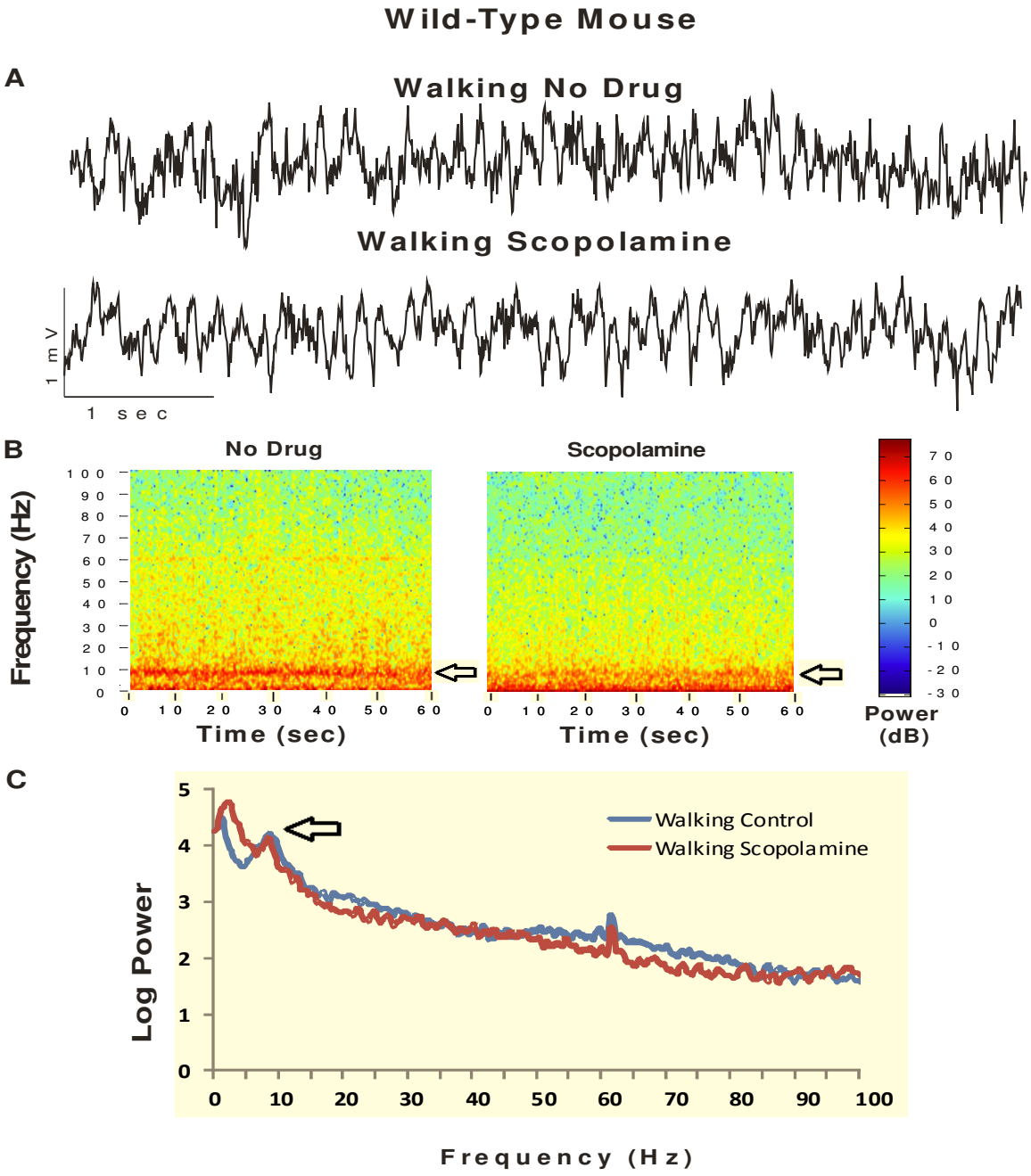

Figure 9 Effects of administration of scopolamine on hippocampal activation of a representative wild-type mouse during walking. **A)** LFP traces (6 seconds) before and after scopolamine injection. **B)** Time-frequency spectrogram and **C)** Power spectra representation of hippocampal activation of a WT mouse before and after administration of scopolamine. Blue line corresponds to baseline while red line represents post scopolamine. Theta power was decreased significantly after scopolamine injection, but its peak frequency remained quite intact. Scopolamine injection did not significantly change the power of either low or high frequency gamma.

3.2.2 VAChT KD^{HET} mice

Theta rhythm in HET mice was less sensitive to scopolamine as compared to theta in WT mice. Scopolamine injection failed to abolish the awake-immobility theta rhythm in HET mice; however, both peak frequency and power of theta were significantly attenuated (Fig. 10). The lack of scopolamine sensitivity of awake-immobile theta rhythm in the hippocampus of HET mice was different from WT mice (3.2.1). Theta peak frequency was reduced from 4.92 ± 0.03 Hz to 3.49 ± 0.21 Hz (n = 6, $P < 0.01$; Fig. 14). Scopolamine suppressed the power of theta rhythm during both immobility and walking (awake-immobility: before scopolamine: 0.40 ± 0.02 log units, after scopolamine 0.17 ± log units, n = 6, $P < 0.001$; walking: 0.37 ± 0.02 log units while baseline power was 0.89 ± 0.04 log units, n = 6, $P < 0.0001$; Fig 14-15). Similar to WT mice, the walking theta peak frequency was not changed significantly by scopolamine (7.96 ± 0.32 Hz, report baseline again n = 6, $P = 0.32$; Fig. 15). As observed for the WT mice, injection of scopolamine to HET mice also did not alter the power of low frequency gamma during awake-immobility or walking (2-way repeated measures ANOVA, n = 6 mice, $F_{(1, 10)} = 1.33$, $P = 0.28$; Fig. 10-11, 14-15). High frequency gamma power also did not change significantly after scopolamine during awake-immobility (1.73 ± 0.12 log units) or during walking (1.94 ± 0.12 log units; 2-way ANOVA, n = 6, 2-way repeated measures ANOVA $F_{(1, 10)} = 0.05$, $P = 0.82$; Fig. 10-11, 14-15).

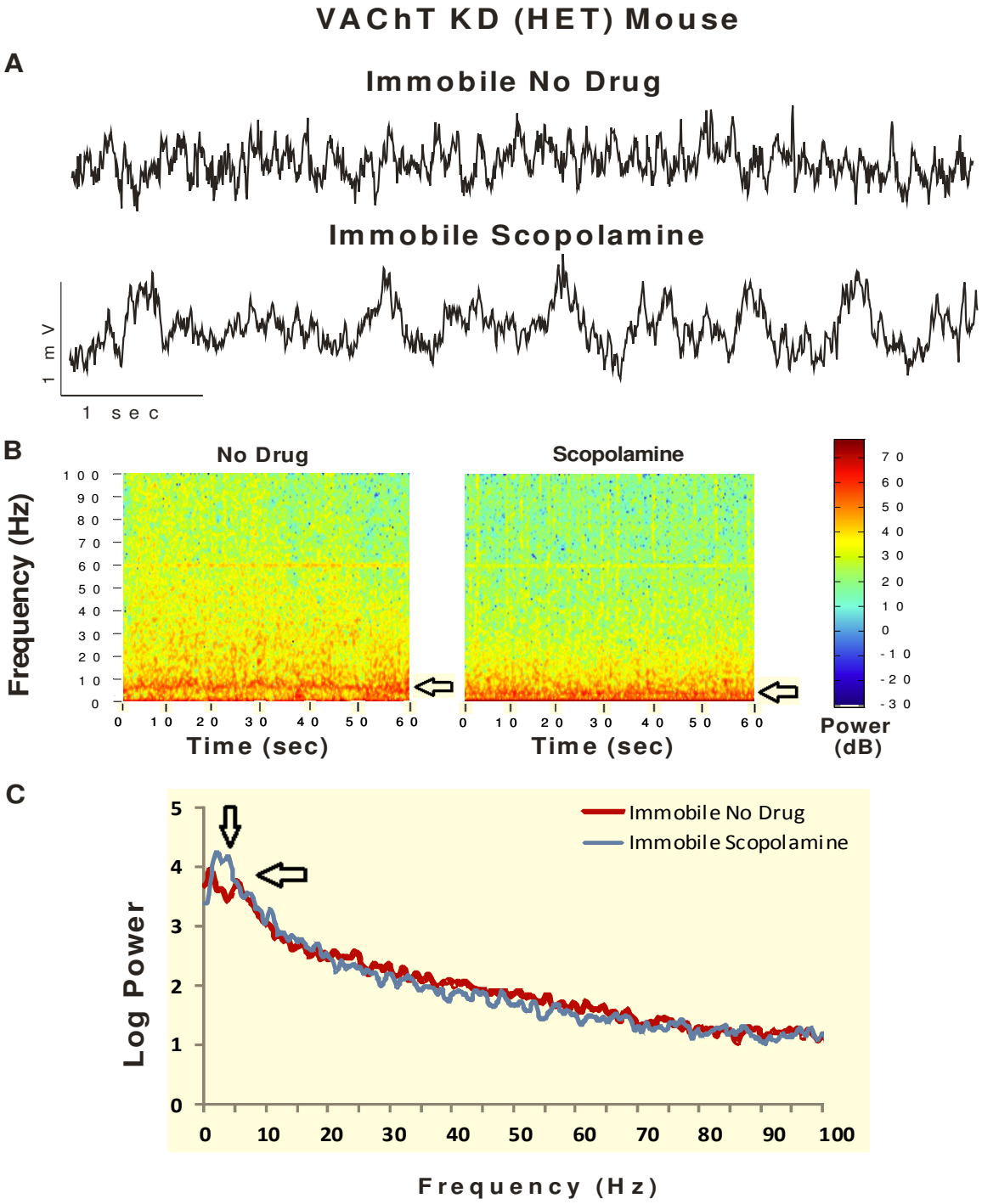

Figure 10 Effects of administration of scopolamine on hippocampal activation of a representative VAChT KD^{HET} mouse during awake-immobility. **A)** LFP traces (6 seconds) before and after scopolamine injection. **B)** Time-frequency spectrogram and **C)** Power spectra before (red trace) and after administration of scopolamine (blue trace). Scopolamine injection shifted the theta peak to a lower frequency and reduced its power. Scopolamine did not change significantly the low- and high-frequency gamma power.

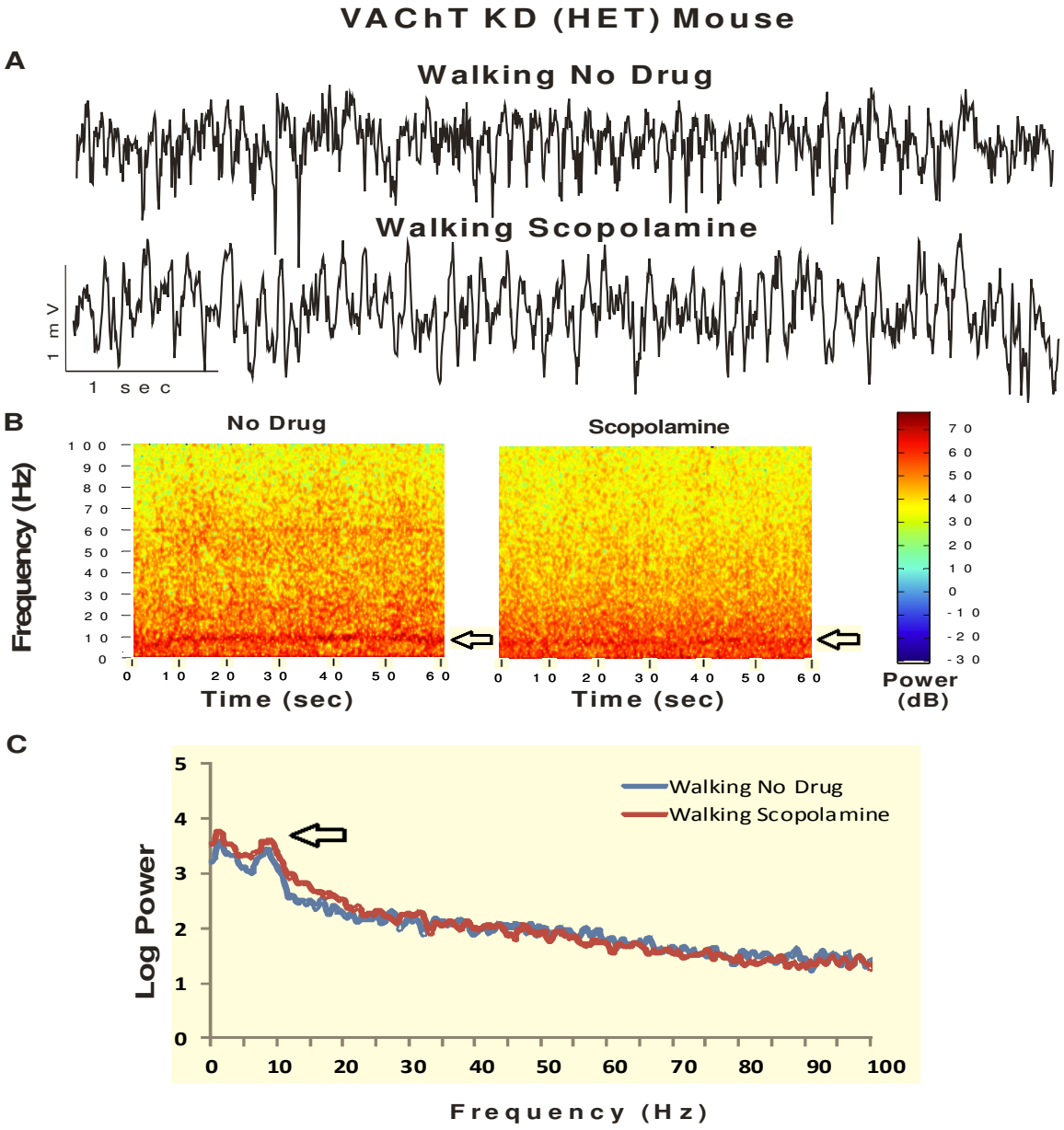

Figure 11 Effects of administration of scopolamine on hippocampal activation of a representative VAChT KD^{HET} mouse during walking. **A)** LFP traces (6 seconds) before and after scopolamine injection. **B)** Time-frequency spectrogram and **C)** Power spectra representation of hippocampal activation of a HET mouse before and after administration of scopolamine. Blue line corresponds to baseline while red line represents post scopolamine. Although power of theta rhythm was significantly suppressed after scopolamine injection, its peak frequency remained quite intact. Scopolamine injection did not significantly change the power of either low- or high-frequency gamma.

3.2.3 VAChT$^{Nkx2.1\text{-}Cre\text{-}flox/flox}$ mice

Sensitivity of hippocampal LFPs to scopolamine was similar in KO and WT mice. Theta generated during awake-immobility was abolished by scopolamine injection (Fig. 12). Walking-induced theta peak did not change significantly after administration of scopolamine (7.79 ± 0.21 Hz, n = 6, P = 0.71, paired t-test; Fig. 13, 15). Unlike in WT and HET mice, power of walking-induced theta was not suppressed significantly post scopolamine injection (0.83 ± 0.08, n = 6, P = 0.21, paired t-test; Fig. 13, 15). Scopolamine also failed to alter the power of low-frequency gamma generated during awake-immobility (2.64 ± 0.13 log units; Fig. 14). A similar result was observed for the walking-induced low-frequency gamma (2.93 ± 0.15 log units, n = 6, $F_{(1, 10)}$ = 0.19, P = 0.67; Fig. 15). High-frequency gamma during awake-immobility showed a non-significant increase of power after scopolamine (1.87 ± 0.12 log units, n = 6; Fig. 12, 14). Scopolamine injection did not change the power of walking-induced high frequency gamma (2.16 ± 0.13 log units, n = 6, $F_{(1, 10)}$ = 0.36, P = 0.56; Fig. 13, 15).

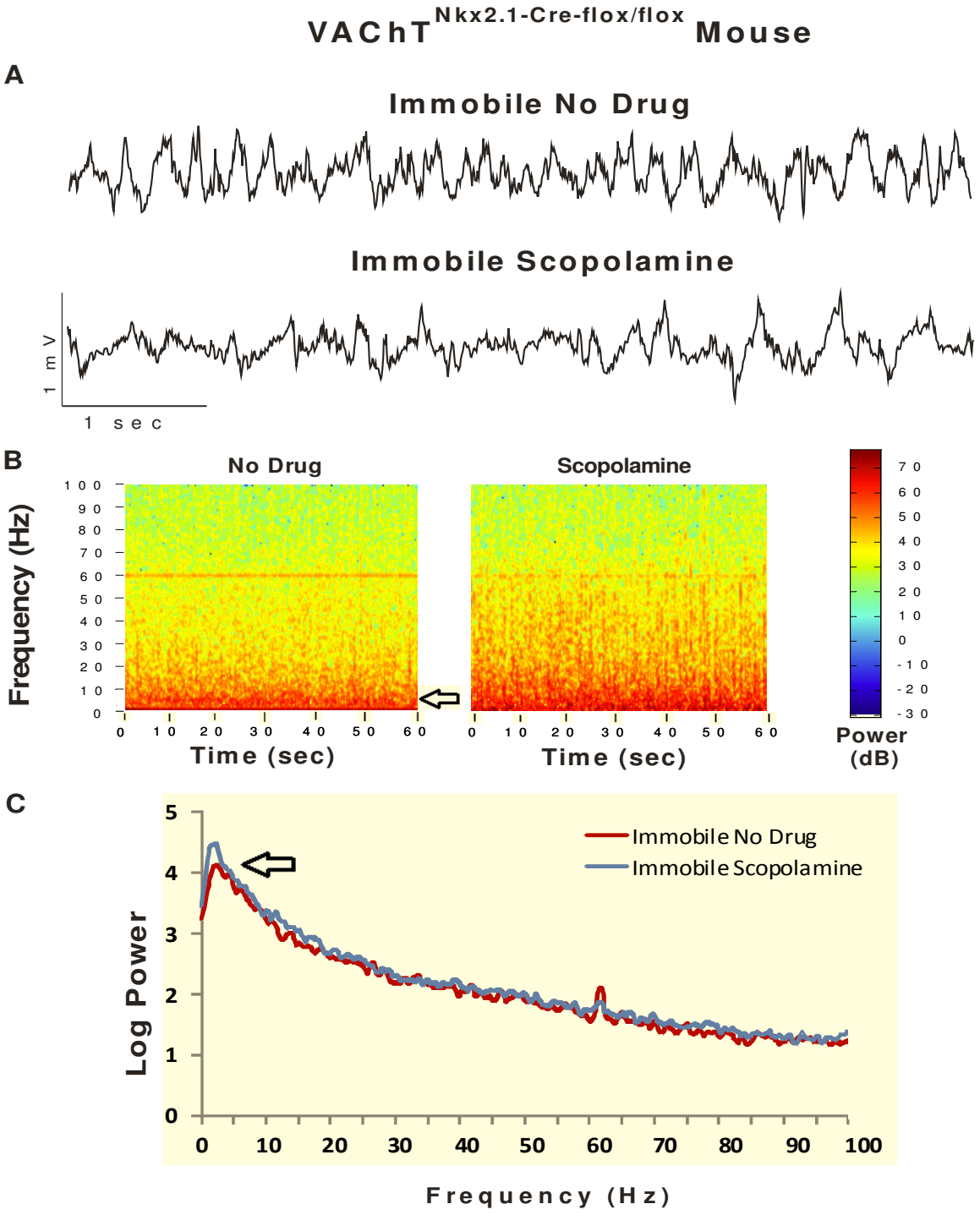

Figure 12 Effects of administration of scopolamine on hippocampal activation of a representative VAChT$^{Nkx2.1\text{-}Cre\text{-}flox/flox}$ mouse during awake-immobility. **A)** LFP traces (6 seconds) before and after scopolamine injection. **B)** Time-frequency spectrogram and **C)** Power spectra before (red trace) and after administration of scopolamine (blue trace). Scopolamine injection abolished the theta peak during awake-immobility, but did not change significantly the low- and high-frequency gamma power.

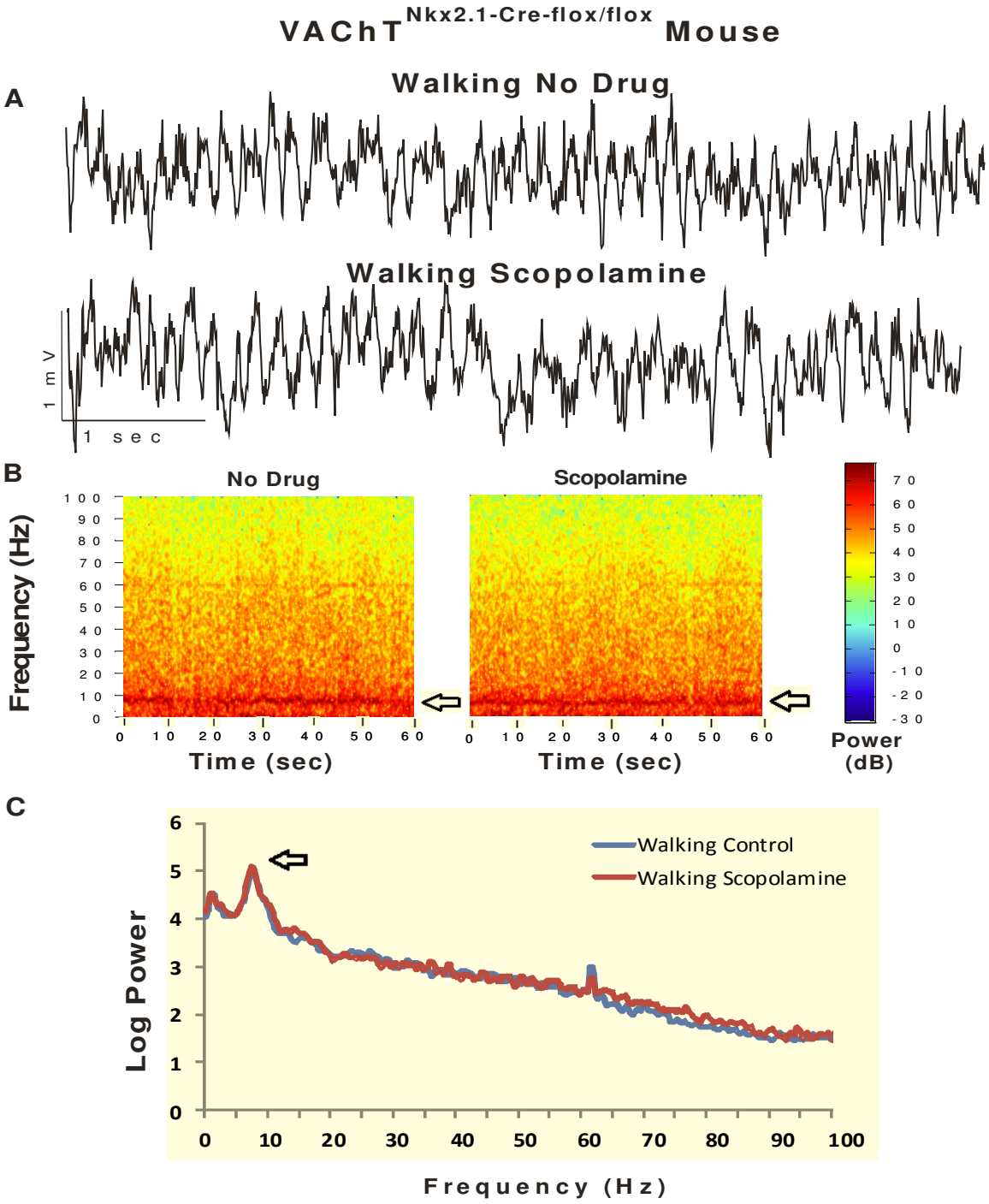

Figure 13 Effects of administration of scopolamine on hippocampal activation of a representative VAChT$^{Nkx2.1\text{-}Cre\text{-}flox/flox}$ mouse during walking. **A)** LFP traces (6 seconds) before and after scopolamine injection. **B)** Time-frequency spectrogram and **C)** Power spectra representation of hippocampal activation of a KO mouse before and after administration of scopolamine. Blue line corresponds to baseline while red line represents post scopolamine. Injection of scopolamine failed to alter any of the four variables significantly.

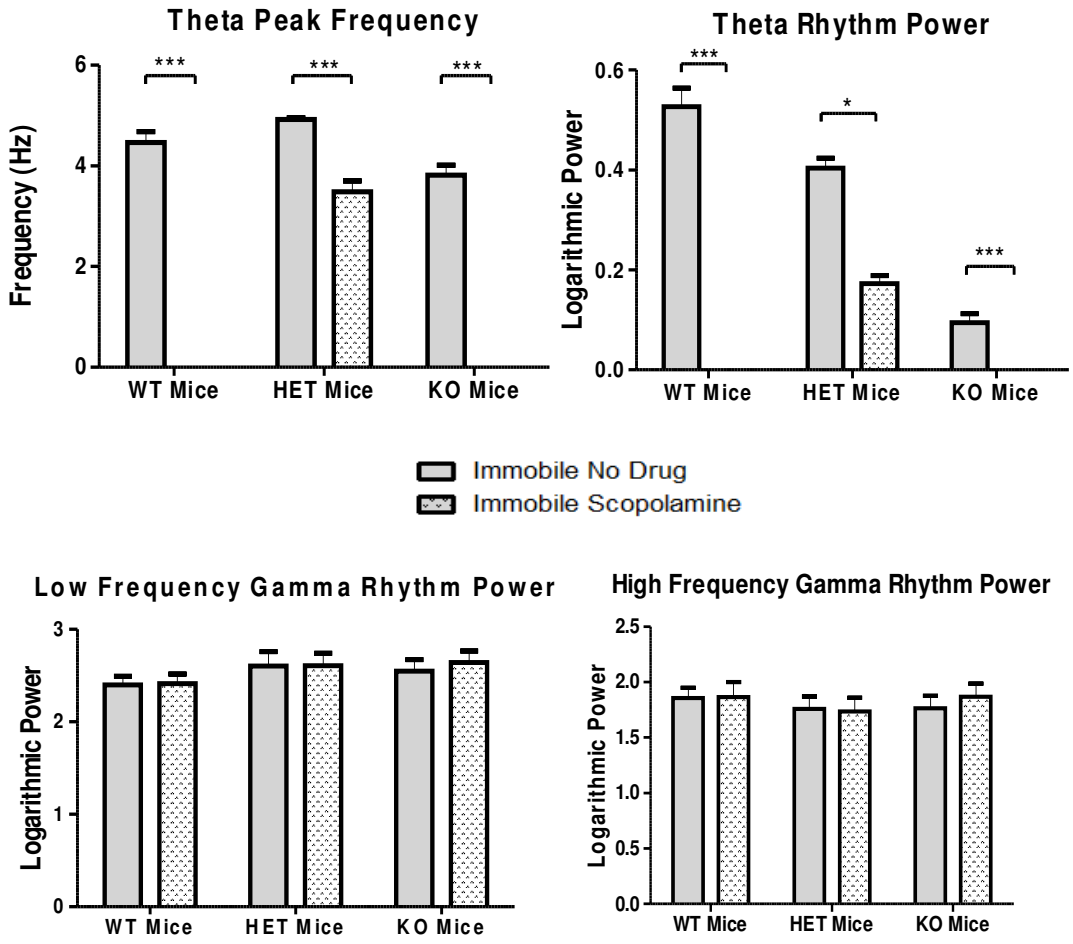

Figure 14 Effect of scopolamine on hippocampal activation of WT (n = 6), HET (n = 6), and KO (n = 6) mice during awake-immobility. Values are expressed as mean ± SEM. * $P<0.05$, *** $P<0.001$: difference between no drug and scopolamine using repeated measures two-way ANOVA followed by Bonferroni test. Scopolamine abolished theta peak frequency and power in WT and KO mice, and attenuated theta frequency and powerin HET mice. No significant change was noticed in power of gamma in any mouse groups after scopolamine.

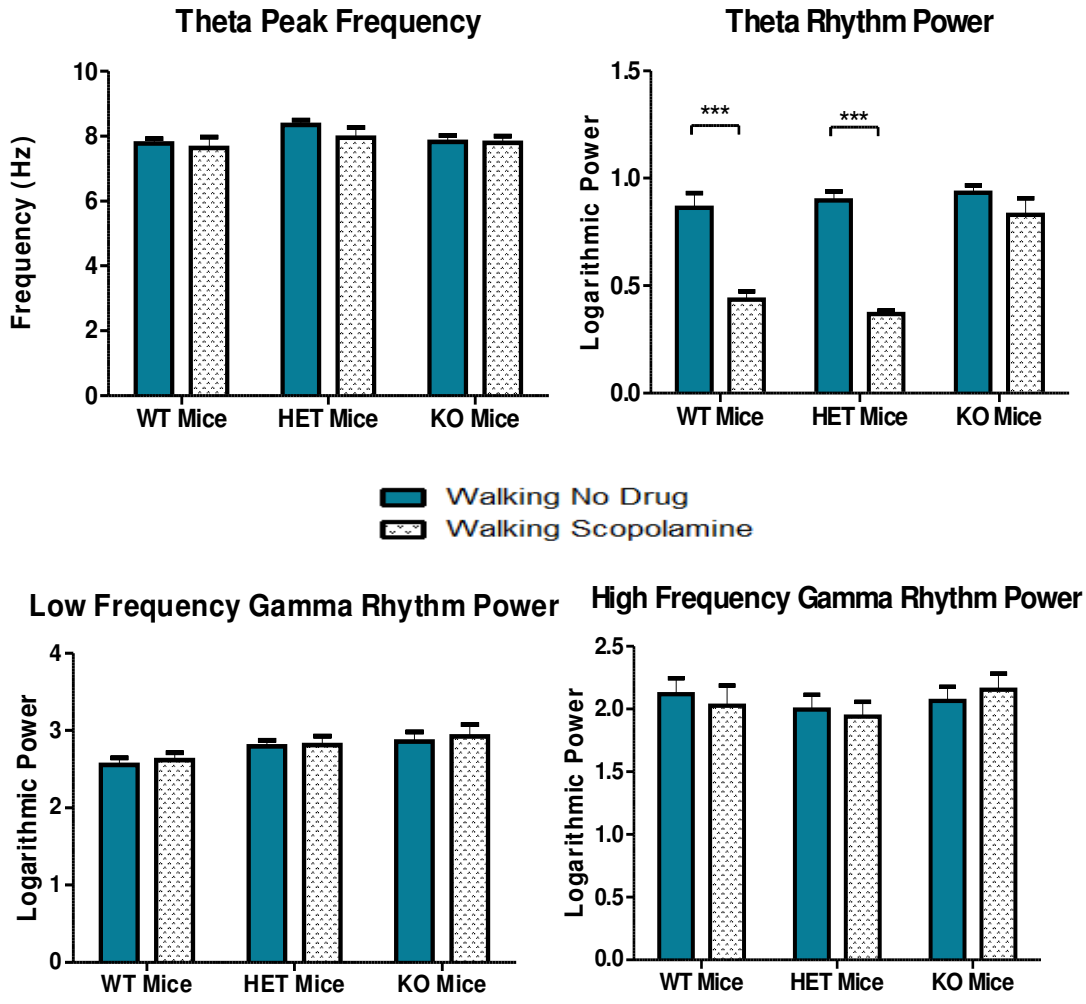

Figure 15 Effect of scopolamine on hippocampal activation of WT (n = 6), HET (n = 6), and KO (n = 6) mice during walking. Values are expressed as mean ± SEM. *** $P<0.001$: difference between no drug and scopolamine using repeated measures two-way ANOVA followed by Bonferroni test. Theta peak frequency did not change significantly. Theta power attenuated in WT and HET mice but not in KO mice. Scopolamine failed to alter the power of gamma oscillations in all three groups during walking.

3.3 CPP injection

To investigate the source of compensation which might have happened in HET mice, the NMDA receptor antagonist 3-[(R)-2-carboxypiperazin-4-yl]-prop-2-enyl-1-phosphonic acid (CPP) was injected (10 mg/kg i.p.) to mice from all groups. The LFPs were recorded from mice 30 minutes post injection.

3.3.1 Wild-type mice

CPP injection did not alter the awake-immobile theta peak frequency significantly (3.98 ± 0.21 Hz, n = 6, $P = 0.13$); however, walking-induced theta peak frequency was suppressed significantly (7.01 ± 0.30 Hz, n = 6, $P < 0.05$) as compared to baseline (7.83 ± 0.20 Hz). Power of theta was significantly suppressed during awake-immobility and walking after injection of CPP (awake-immobility: 0.38 ± 0.04 log units, n = 6, $P < 0.05$; walking: 0.24 ± 0.03 log units, n = 6, $P < 0.001$). No significant change was observed post CPP injection in the power of low frequency gamma oscillations during either of the behaviors (awake-immobility: 2.40 ± 0.1 log units; walking: 2.55 ± 0.09; 2-way ANOVA, n = 6, $F_{(1, 10)} = 0.15$, $P = 0.70$; Fig. 16-17, 22-23). There was a non-significant increase in power of high frequency gamma during awake-immobility (1.86 ± 0.09 log units; Figure 16, 22). Power of high frequency gamma after CPP injection during walking was 2.09 ± 0.16 log units, which did not differ from baseline significantly (2-way ANOVA, n = 6, $F_{(1, 10)} = 0.05$, $P = 0.84$; Fig. 17, 23).

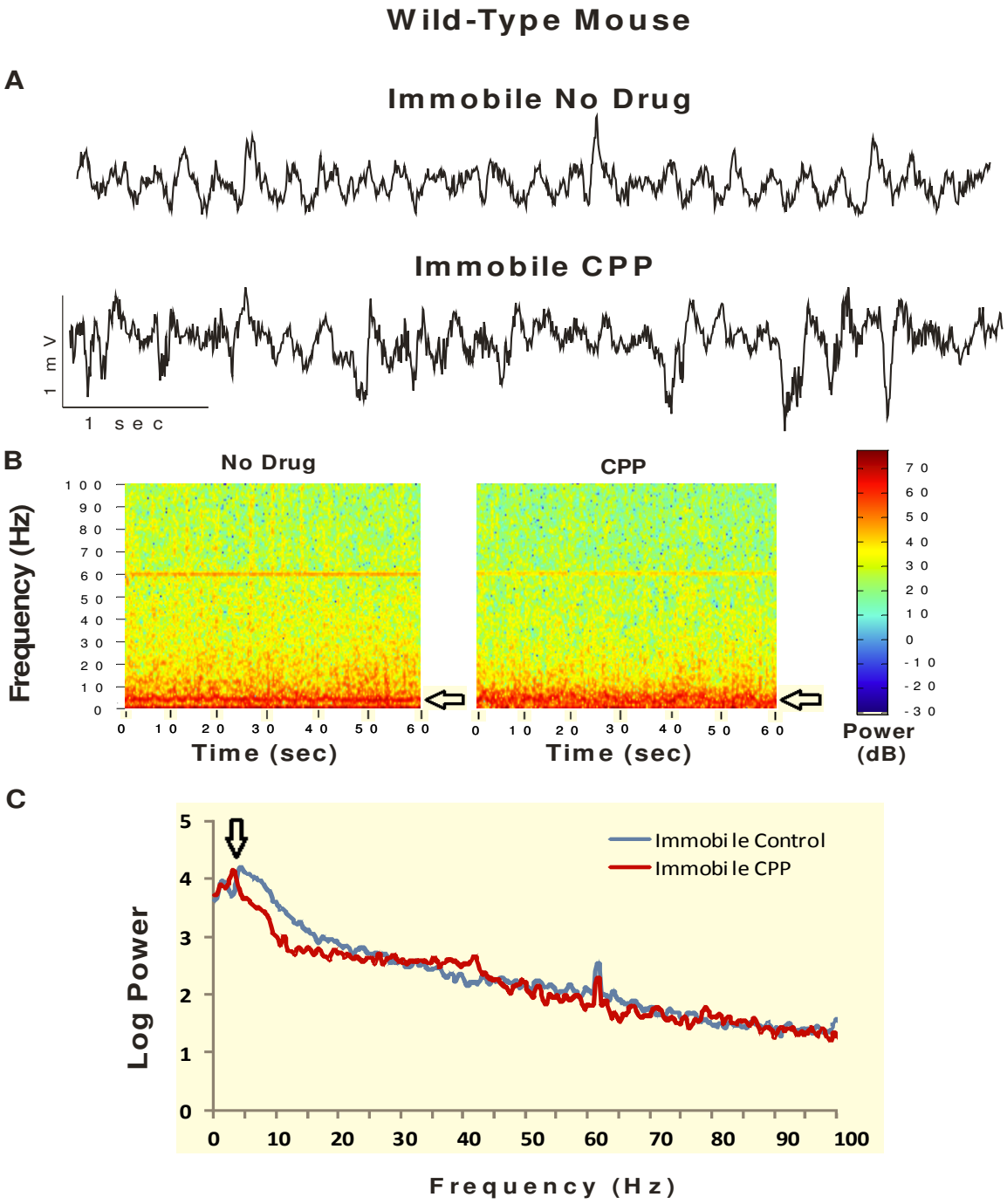

Figure 16 CPP injection and hippocampal activation in a Wild-Type mouse during awake-immobility. **A)** LFP traces (6 seconds) before and after CPP injection. **B)** Time-frequency spectrogram and **C)** Power spectra representation of hippocampal activation of a WT mouse before and after administration of CPP. Blue line corresponds to baseline while red line represents post CPP. Power of theta rhythm but not theta peak frequency was suppressed significantly by CPP. CPP injection did not significantly change the power of either low- or high-frequency gamma.

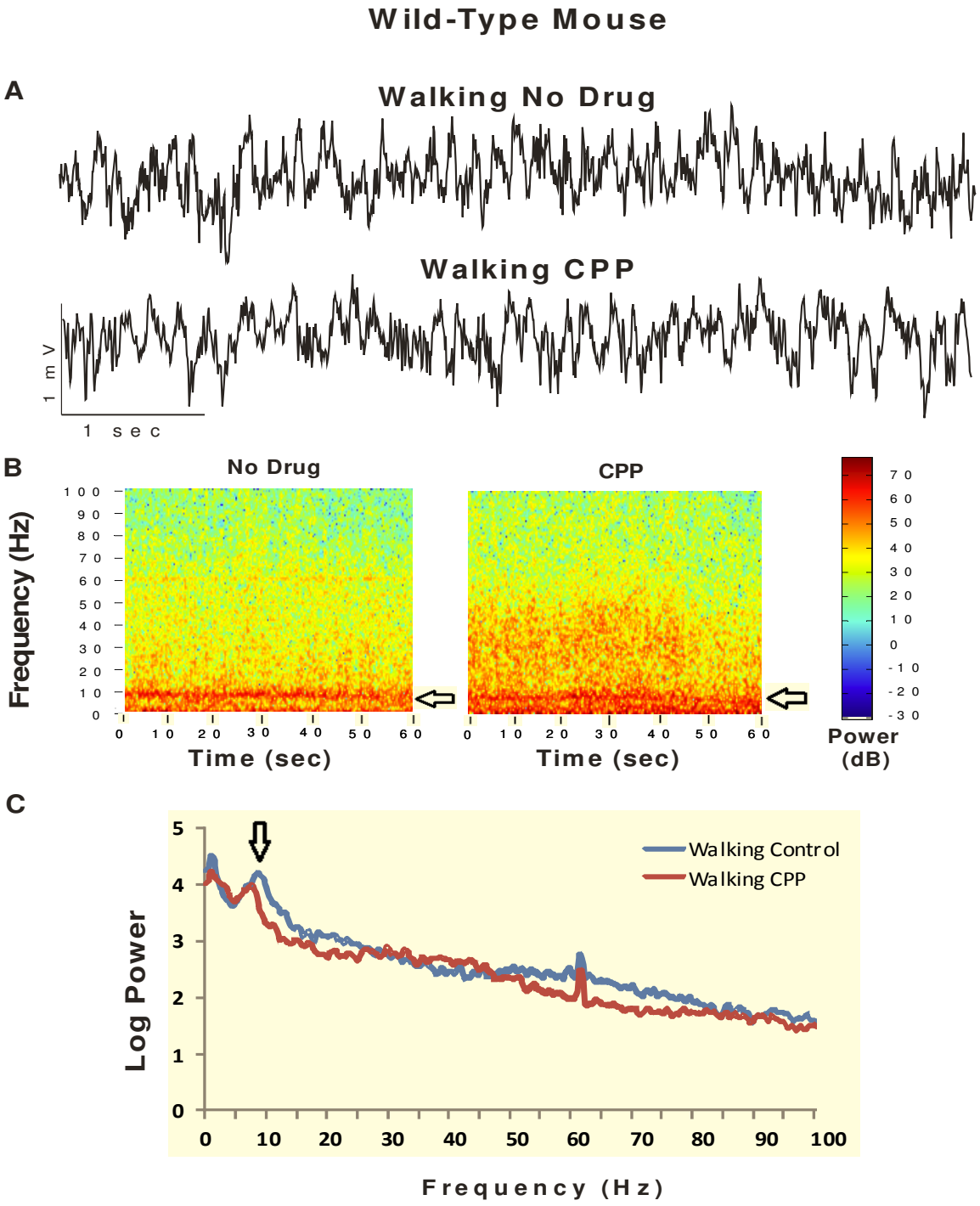

Figure 17 CPP injection and hippocampal activation in a Wild-Type mouse during walking. **A)** LFP traces (6 seconds) before and after CPP injection. **B)** Time-frequency spectrogram and **C)** Power spectra representation of hippocampal activation of a WT mouse before and after administration of CPP. Blue line corresponds to baseline while red line represents post CPP. CPP suppressed both power and peak frequency of theta rhythm significantly, but it did not significantly change the power of either low- or high-frequency gamma.

3.3.2 VAChT KD^{HET} mice

Administration of CPP abolished the awake-immobility theta rhythm. A theta peak, as indicated by rise of the theta peak, was not detected in any of the six HET mice during awake-immobility (Fig. 18). CPP shifted the walking-induced theta rhythm peak to a significantly lower frequency (7.59 ± 0.28 Hz; n = 6, $P < 0.05$, paired t-test; Fig. 19, 22). Furthermore, power of theta recorded during walking was significantly attenuated (3.53 ± 0.02 log units; n = 6, $P < 0.0001$, paired t-test; Fig. 19, 23). Similar to WT mice, low-frequency gamma power in HET mice did not change significantly post CPP (awake-immobility: 2.60 ± 0.15 log units; walking: 2.79 ± 0.08 log units; 2-way ANOVA, n = 6, $F_{(1, 10)} = 0.40$, $P = 0.54$; Fig. 18-19, 22-23). When compared to baseline recording, power of high frequency gamma was not altered significantly post CPP injection (awake-immobility: 1.96 ± 0.15 log units; walking: 2.11 ± 0.14 log units; 2-way repeated measures ANOVA, n = 6, $F_{(1, 10)} = 0.61$, $P = 0.45$; Fig. 18-19, 22-23).

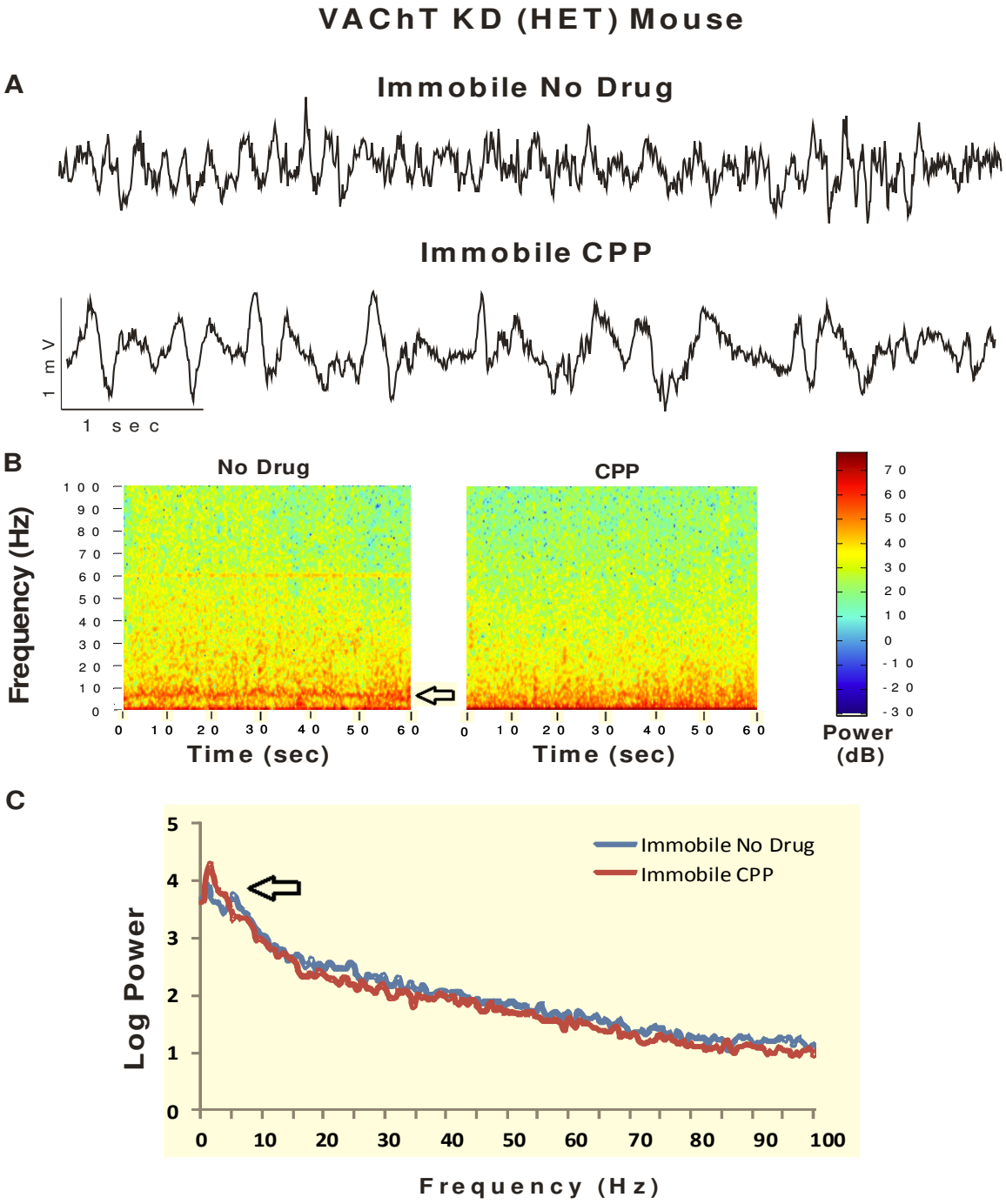

Figure 18 CPP injection and hippocampal activation in a VAChT KD^{HET} mouse during awake-immobility. **A)** LFP traces (6 seconds) before and after CPP injection. **B)** Time-frequency spectrogram and **C)** Power spectra before (blue trace) and after administration of CPP (red trace). CPP injection abolished the theta peak during awake-immobility, but did not change significantly the low- and high-frequency gamma power.

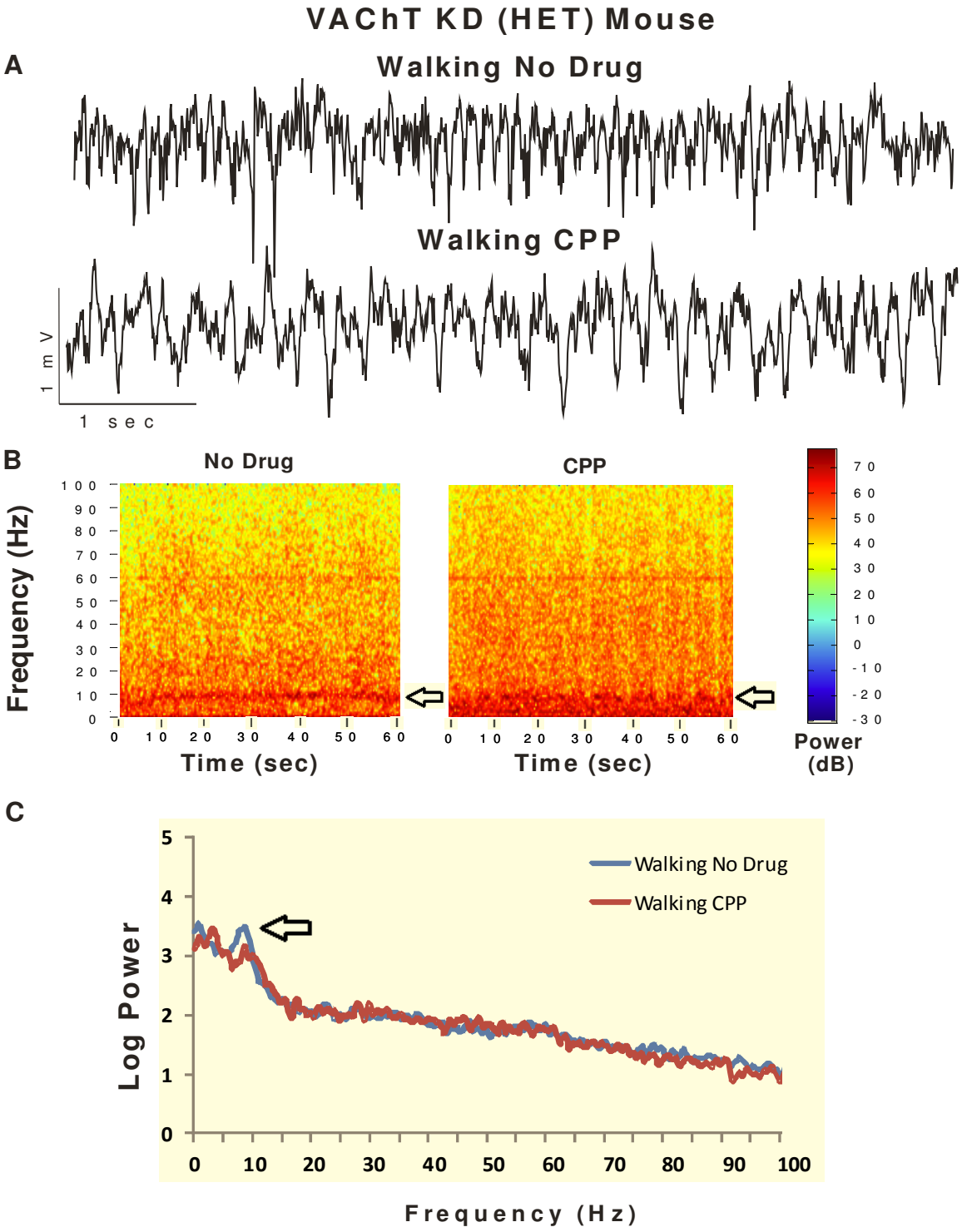

Figure 19 CPP injection and hippocampal activation in a VAChT KD^{HET} mouse during walking. **A)** LFP traces (6 seconds) before and after CPP injection. **B)** Time-frequency spectrogram and **C)** Power spectra before (blue trace) and after administration of CPP (red trace). CPP injection significantly attenuated the power of theta. Theta peak shifted to a lower frequency. CPP failed to change the low- and high-frequency gamma power.

3.3 VAChT$^{Nkx2.1\text{-}Cre\text{-}flox/flox}$ mice

CPP injection did not change the peak frequency of awake-immobility theta in the KO (VAChT$^{Nkx2.1\text{-}Cre\text{-}flox/flox}$) mice (4.04 ± 0.19 Hz, n = 6, $P = 0.43$), but it significantly reduced the walking theta frequency (6.91 ± 0.12 Hz, n = 6, $P < 0.01$). In contrast to WT mice, CPP failed to alter the theta power during awake-immobility (0.069 ± 0.02 log units, n = 6, $P = 0.35$). However, theta power during walking (0.29 ± 0.03 log units) was suppressed significantly (n = 6, $P < 0.0001$). Average logarithmic power of low-frequency gamma rhythm was 2.55 ± 0.12 log units during awake-immobility and 2.86 ± 0.12 log units while walking (Fig. 22-23). Similar to WT mice, power of both low- and high-frequency gamma did not change significantly during awake-immobility or walking in response to CPP injection.

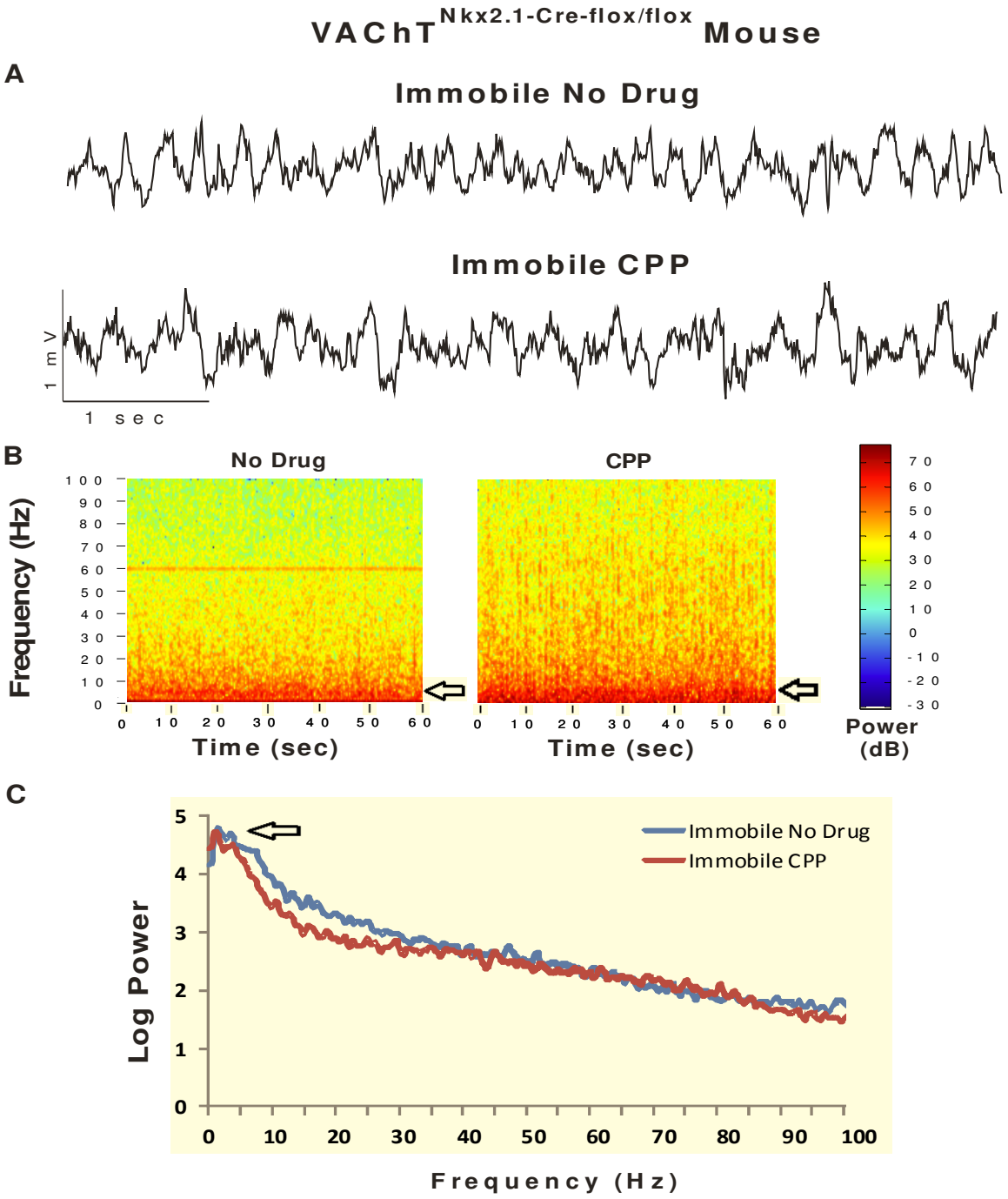

Figure 20 CPP injection and hippocampal activation in a VAChT$^{Nkx2.1\text{-}Cre\text{-}flox/flox}$ mouse during awake-immobility. **A)** LFP traces (6 seconds) before and after CPP injection. **B)** Time-frequency spectrogram and **C)** Power spectra representation of hippocampal activation of a KO mouse before and after administration of CPP. Blue line corresponds to baseline while red line represents post CPP. Injection of CPP failed to alter any of the four variables significantly.

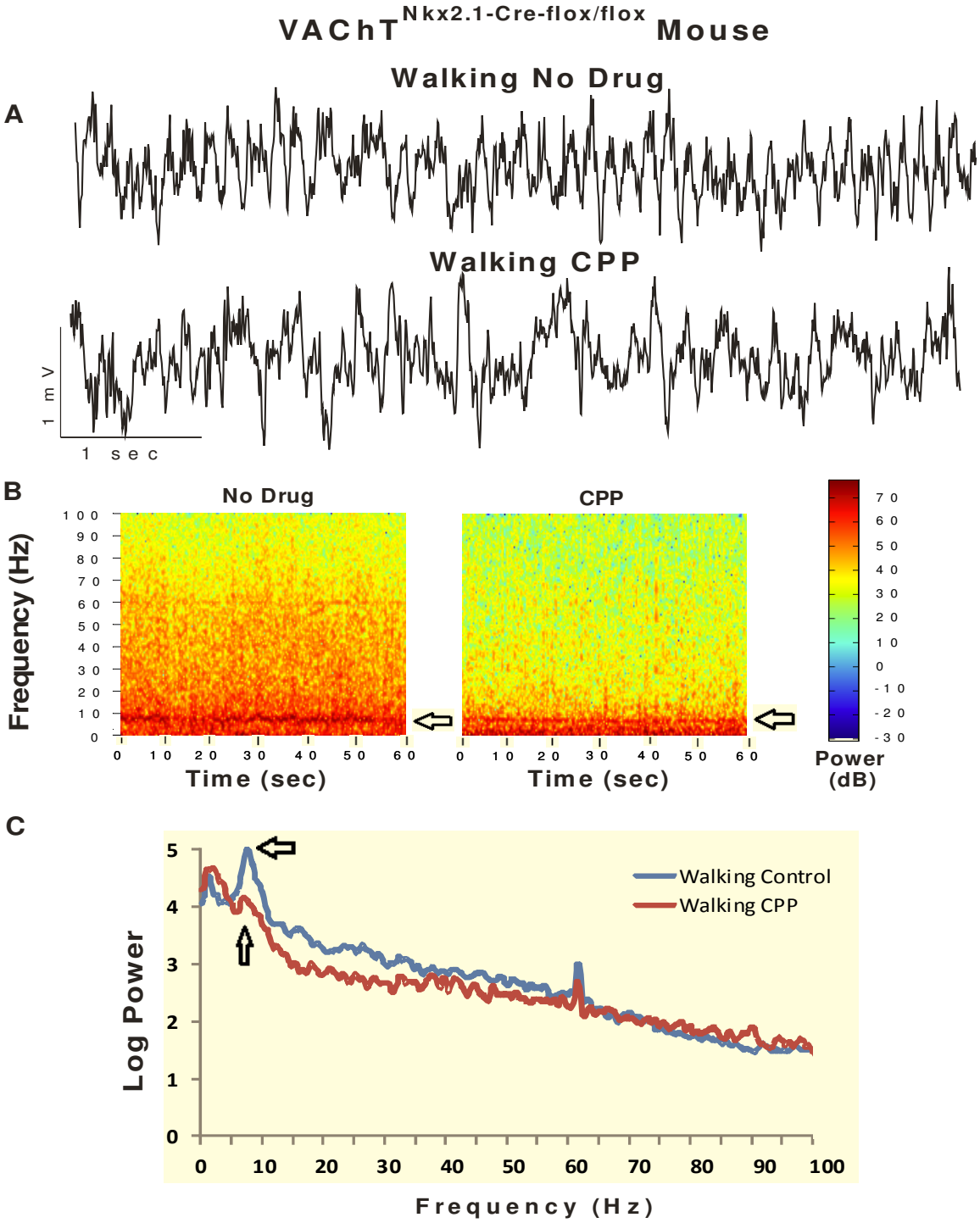

Figure 21 CPP injection and hippocampal activation in a VAChT$^{Nkx2.1\text{-}Cre\text{-}flox/flox}$ mouse during walking. **A)** LFP traces (6 seconds) before and after CPP injection. **B)** Time-frequency spectrogram and **C)** Power spectra before (blue trace) and after administration of CPP (red trace). CPP injection significantly attenuated the power of theta. Theta peak shifted to a lower frequency. CPP significantly suppressed the power of low-frequency gamma power but not high-frequency gamma power.

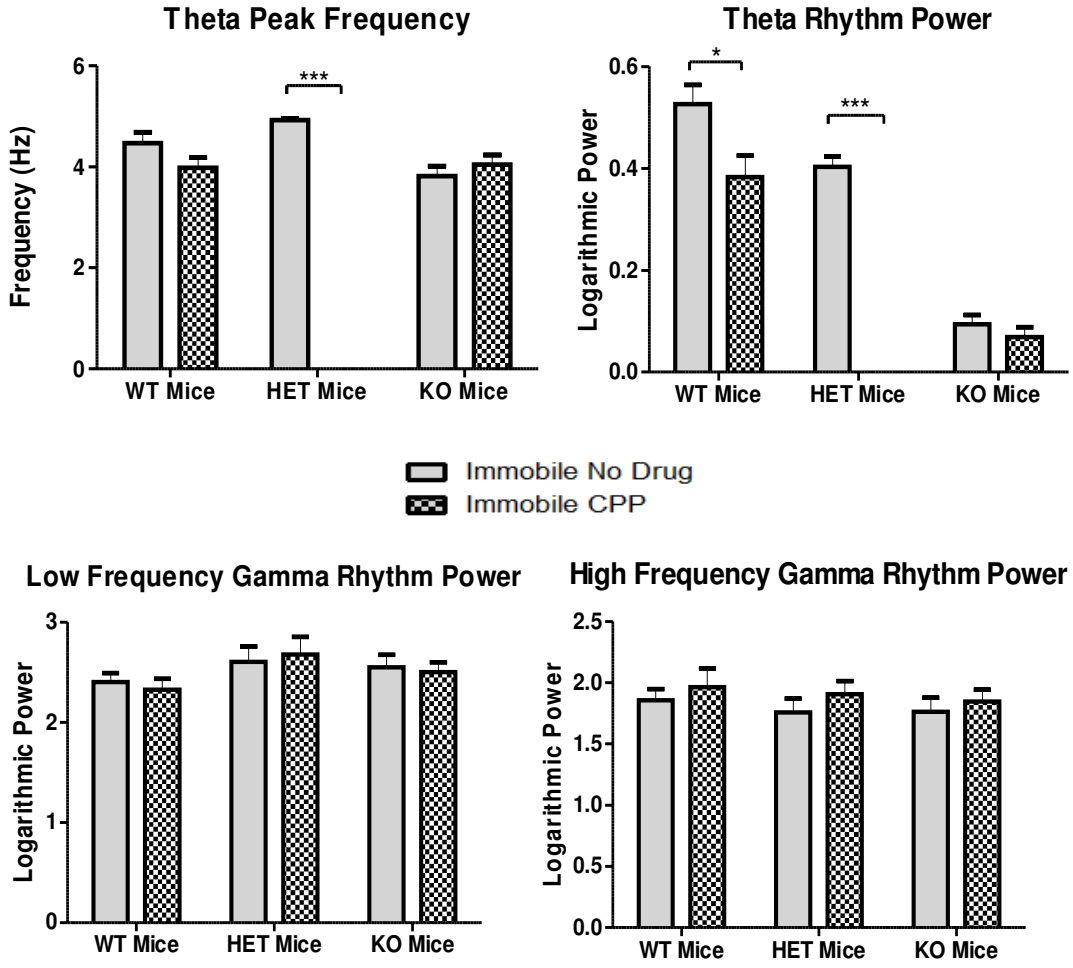

Figure 22 Effect of CPP on hippocampal activation of WT (n = 6), HET (n = 6), and KO (n = 6) mice during awake-immobility. Values are expressed as mean ± SEM. * $P<0.05$, *** $P<0.001$. Repeated measures two-way ANOVA (behavior x drug) followed by Bonferroni test was used. *WT Mice*: Theta power attenuated while its peak frequency did not change significantly. CPP injection failed to alter the power of gamma oscillations. *HET Mice*: Immobile theta peak was not observed, thus zero theta power, and the power of low- and high-frequency gamma was not significantly changed after CPP. *KO Mice*: None of the four variables changed significantly after injection of CPP.

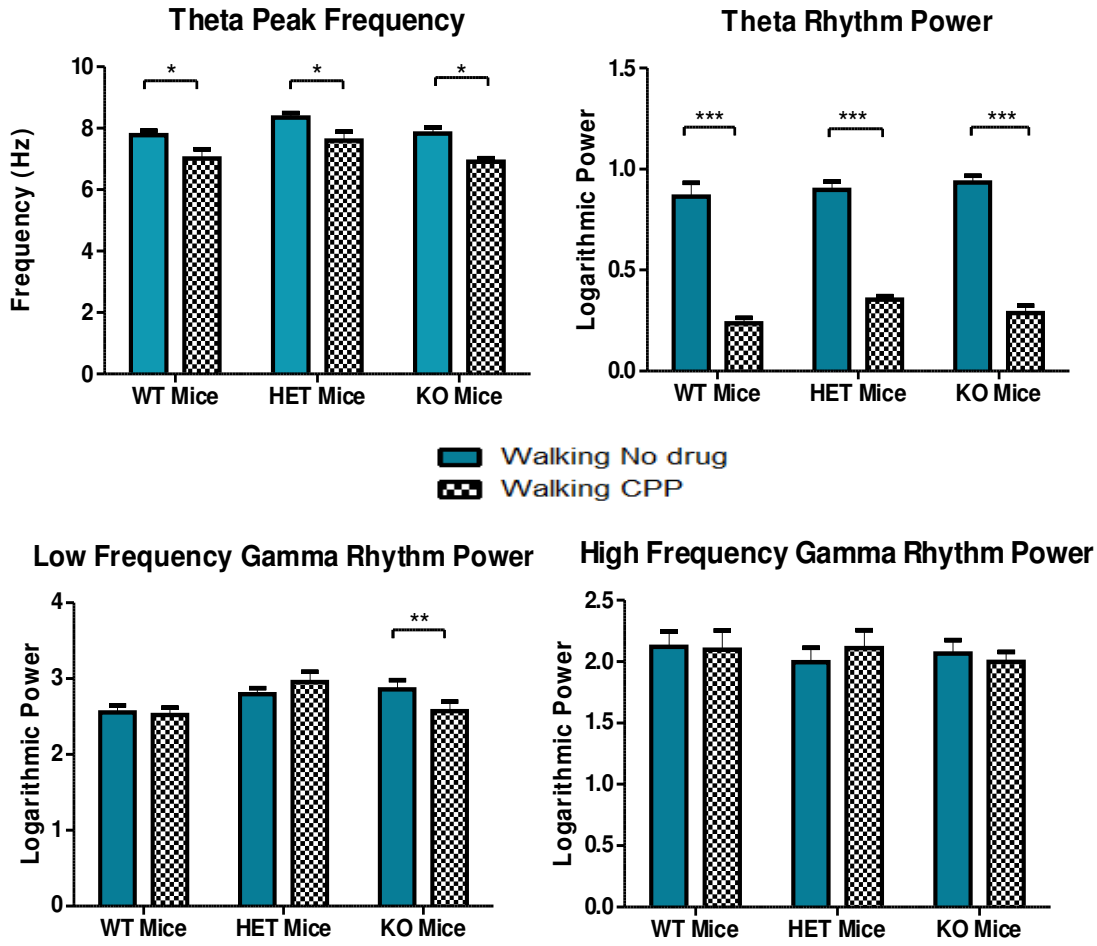

Figure 23 Effect of CPP on hippocampal activation of WT (n = 6), HET (n = 6), and KO (n = 6) mice during walking. Values are expressed as mean ± SEM. * $P<0.05$, ** $P<0.01$, *** $P<0.001$. Repeated measures two-way ANOVA (behavior x drug) followed by Bonferroni test was used. In all three groups of mice, theta power was strongly attenuated after injection of CPP. Theta peak also shifted to a significantly lower frequency in all groups. Although CPP suppresses the low-frequency gamma power in KO mice, no significant reduction was noticed in WT and HET mice. Power of high-frequency gamma did not vary significantly in any of the three groups after administration of CPP.

4 Discussion

4.1 Hippocampal activation during awake-immobility

My results indicate that two types of theta rhythm are generated within the hippocampus based on the behavior. This is consistent with previous findings (Vanderwolf, 1969; Vanderwolf, 1975; Leung et al., 1982; Oddie and Bland, 1998; Bland and Oddie, 2001). Theta rhythm generated during awake-immobility in all groups of mice had significantly lower peak frequency and power as compared with the walking induced theta. No significant difference was found in the power of either low- or high-frequency gamma activity between groups during awake-immobility.

Vanderwolf (1988) suggested that different neurotransmitters regulate generation of each type of theta rhythm. Multiple studies using cholinergic agonist and antagonist drugs showed that acetylcholine (ACh) is the neurotransmitter responsible for generation of hippocampal theta rhythm during awake-immobility (Sainsbury et al., 1987; Vanderwolf, 1988; Leung 1998; Tai et al., 2011). I found that the power of theta during awake-immobility decreased in the order of Wild-Type, VAChT KD^{HET} and $VAChT^{Nkx2.1\text{-}Cre\text{-}flox/flox}$, which is the order of expected availability of synaptically released acetylcholine in the septohippocampal system This further suggests that cholinergic functionality is necessary for generation of awake-immobility theta.

The awake-immobility theta is also referred to as atropine-sensitive. Injection of scopolamine in all three groups of mice was accompanied by a short period (~5 minutes) of hyperactivity followed by a longer period (~20 minutes) of immobility. My data

showed that administration of scopolamine abolished the theta generated during awake-immobility in Wild-Type and VAChT$^{Nkx2.1\text{-}Cre\text{-}flox/flox}$ mice. Atropine-sensitive theta has been suggested to indicate sensory processing in the hippocampus (Vanderwolf, 1988). Based on this model the atropine-sensitive theta provides sensory information required for the initiation of voluntary movement or signal the intensity of an upcoming movement. This is consistent with the sensorimotor integration model proposed by Bland and Oddie (2001).

Despite the fact that VAChT was deleted from basal forebrain of the VAChT$^{Nkx2.1\text{-}Cre\text{-}flox/flox}$ mice (Al-Onaizi, under review), a low power theta was still present during awake-immobility. Two reasons could account for this result. First, some ACh is still being released in the septo-hippocampal pathway in these forebrain-VAChT knockout mice, despite near zero VAChT levels assessed by protein and mRNA (Al-Onaizi, under review). Next, cholinergic neurons projecting from pedunculopontine tegmental nucleus (PPT) to the medial septum (MS) play a role in generation of atropine-sensitive theta. Direct application of atropine to the MS eliminated the atropine-sensitive theta rhythm in the hippocampus in the rat under urethane anesthesia (Stewart and Fox, 1989), which may block muscarinic cholinergic synapses on GABAergic septohippocampal neurons (Alreja et al., 2000; Wu et al., 2000). Stimulation of PPT or infusion of cholinergic agonists into the PPT has been shown to induce hippocampal theta (Vertes, 1982; Vertes et al., 1993).

Another interesting result was the failure of scopolamine injection in totally abolishing the atropine-sensitive theta in VAChT KD^{HET} mice. Administration of scopolamine suppressed the theta power significantly and shifted the peak to a lower

frequency but failed to abolish it. This suggests that a compensatory mechanism might have developed in these mice. Based on the model proposed by Colom (2006), septohippocampal cholinergic neurons, in addition to septohippocampal glutamaterigc neurons, help to increase the level of excitation within the medial septum to a threshold necessary for oscillation in theta frequency. It is possible that the septohippocampal glutamatergic neurons release more glutamate in order to compensate for the cholinergic deficiency.

In another study by Allen et al., (2006), cholinergic basal forebrain neurons (in vitro) were shown to be capable of releasing glutamate as a co-transmitter. Co-release of glutamate was subjected to the negative-feedback inhibition regulated by the M2 subtype muscarinic cholinergic receptors located presynatically. Prado et al., 2006 reported that release of ACh was reduced to ~33% in VAChT KD^{HET} mice. In VAChT KD^{HET} mice, decreased release from basal forebrain cholinergic neurons may result in less feedback inhibition through M2 receptors, and more glutamate being co-released.

Thus, I predict that, decreasing cholinergic tone may trigger the glutamatergic neurons to increase their activity or enhance the release of glutamate from basal forebrain cholinergic neurons. In agreement with this, NMDA receptor antagonist CPP abolished the awake-immobility theta in VAChT KD^{HET} mice, and not other groups of mice. In contrast, immobility theta in wildtype and $VAChT^{Nkx2.1\text{-}Cre\text{-}flox/flox}$ mice was not significantly affected after CPP injection. Other than expecting to block glutamatergic NMDA receptor-mediated synaptic transmission in the hippocampus, CPP is expected to block NMDA receptors mediated by septo-hippocampal glutamatergic neurons synapsing on both hippocampal and medial septal neurons, and glutamatergic neurons projecting

from SUM directly to the hippocampus (Kiss et al., 2000) and indirectly to the medial septum (Vertes, 1992; Borhegyi et al., 1998). The nature of compensation that may have happened in these SUM, septohippocampal, or hippocampal glutamatergic neurons remains to be studied.

4.2 Hippocampal activation during walking

Theta power during walking did not show a significant difference among the different VAChT mutants, suggesting that the amplitude of walking-induced theta might be mainly mediated by non-cholinergic neurons. GABAergic (Stewart and Fox, 1990; Yoder and Pang, 2005; Simon et al., 2006, Borhegyi et al., 2006) and glutamatergic (Leung and Desborough, 1988; Leung and Shen, 2004) septo-hippocampal inputs may maintain the theta rhythmicity during voluntary movements. In addition to septo-hippocampal inputs, serotonin may mediate walking induced theta (Vanderwolf, 1988).

My study showed a decrease in walking-induced theta power following scopolamine injection in Wild-Type and VAChT KD^{HET} mice but not in $VAChT^{Nkx2.1\text{-}Cre\text{-}flox/flox}$ mice. This result supports the proposal that an atropine-sensitive component is also found in the hippocampal theta rhythm during walking in the wildtype and VAChT KD^{HET} mice (Shin et al., 2005), similar to rats (Vanderwolf, 1988; Leung, 1998; Bland and Oddie, 2001). In a study by Leung (1985), the rise of the theta peak recorded during walking was reduced after atropine. On the other hand, the lack of atropine sensitivity of the walking theta in $VAChT^{Nkx2.1\text{-}Cre\text{-}flox/flox}$ mice may be expected for mice without acetylcholine release in the septohippocampal neurons, and brainstem cholinergic inputs

to the medial septum were apparently not participating in atropine sensitivity during walking.

Power of theta rhythm during walking was suppressed in all groups of mice after injection of CPP, suggesting that glutamate and NMDA receptors have a critical role in the generation of walking induced theta. Injection of NMDA receptor antagonist $_{D}$-2-amino-5-phosphonovaleric acid ($_{D}$-APV) directly to the medial septum suppressed the amplitude of theta significantly (Leung and Shen, 2004). No such reduction was noticed by injection of AMPA receptors antagonist (DNQX) suggesting postsynaptic NMDA receptors in the medial septum control the amplitude of the hippocampal theta rhythm (Leung and Shen, 2004). Other than medial septum, theta recorded in CA1 is partially driven by distal-dendritic excitation of the pyramidal cells by the perforant pathway from the entorhinal cortex (Vanderwolf and Leung, 1983; Leung, 1984). This pathway is mediated by both NMDA and AMPA receptors (Colbert and Levy, 1992) and inactivation of this pathway strongly attenuated theta rhythm (Heynan and Bilkey, 1994). Furthermore, the independent pacemaker in the CA3 (Kocsis et al., 1999), activated by septohippocampal cholinergic neurons, also have a role in generation of theta in CA1 region. APV blocked the theta rhythm induced by cholinergic agonists in CA3 in vitro (Fellous and Sejnowski, 2000).

There may be several reasons why atropine-resistant theta was not totally abolished after CPP injection. First, cholinergic, atropine-sensitive component also drives or facilitates theta during walking (Vanderwolf, 1988; Leung, 1998; Bland and Oddie, 2001). Second, only the NMDA component of normal glutamatergic transmission is blocked, and the non-NMDA component remains intact. In addition, glutamate may only

be one of the more important neurotransmitter mediating the atropine-resistant theta, and other neurotransmitters such as GABA and serotonin may also play a role in generation of the theta rhythm during walking. The medial septum projects GABAergic neurons to the hippocampus. GABA released from these neurons attaches to the GABA-A receptors located postsynaptically on the interneurons. Medial septal injection of muscimol, a GABA-A receptor agonist also attenuated the hippocampal theta amplitude (Bland et al., 1996). Serotonin depletion via selective lesion of median raphe neurons or sectioning of presumed 5-HT pathway to the hippocampus strongly attenuated the power of walking induced theta (Vanderwolf, 1988).

In all three groups of mice studied here, the peak of the theta rhythm shifted to a significantly lower frequency after injection of CPP, while no such effect was observed after administration of scopolamine. Kirk (1998) suggested that the frequency of the theta rhythm is coded downstream to the medial septum, presumably in the SUM. MS-DBB receives phasic information from SUM, the frequency of which determines the frequency of septal bursting and that of hippocampal theta (Kirk, 1998). SUM acts as the intensity/frequency transducer (Kirk, 1998). SUM receives many inputs from the brainstem that are glutamatergic (Kiss et al., 2002). The reduction of theta frequency after CPP might be due to the fact that the NMDA component of these glutamatergic pathways has been disrupted. Theta peak frequency of VAChT KD^{HET} mice was significantly higher than Wild-Type and $VAChT^{Nkx2.1\text{-}Cre\text{-}flox/flox}$ mice which might have resulted from higher glutamatergic release in the SUM or medial septum, as a consequence of low cholinergic presynaptic inhibition (Allen et al., 2006), or as a consequence of compensation during development.

Administration of CPP severely impaired voluntary movement in all three groups, as has been observed after other NMDA receptor antagonists (Leung and Shen, 2004). Mice showed difficulty maintaining balance, moving hind limbs, standing and jumping. These symptoms started to appear almost 45 minutes post injection and they recovered a few hours later. Walking data included in the analysis of my results in the thesis were all recorded before the onset of these symptoms.

4.3 Gamma oscillations

Gamma activity is proposed to be generated by a recurrent inhibition circuit involving pyramidal cells and GABAergic interneurons (Leung, 1982, 1998; Mann et al., 2005), and brainstem input is suggested to increase recurrent inhibitory gain and increase gamma oscillations (Leung, 1982). Power of gamma increased during walking as compared to immobility in mice. The increase of low-frequency (30-70 Hz) gamma power was significant in the two mutant mouse lines but not in Wild-Type mice. High-frequency (70-100 Hz) gamma power increased significantly in all three groups during walking. Stumpf (1965b) showed that 0.75 mg/kg (they did not say i.p. or i.v., but it is common to inject rabbits i.v.) scopolamine did not prevent the evocation of hippocampal gamma activity evoked by brainstem stimulation in immobilized unanesthetized rabbits. In contrast to Stumpf, Leung (1985) reported that atropine caused a decrease in gamma activity in rats. My results indicated that scopolamine failed to change the power of gamma oscillations significantly. This observation was consistent for all three groups of mice both during walking and awake-immobility. My results showed that injection of the NMDA receptor glutamatergic antagonist CPP, failed to change the power of low- and

high-frequency gamma oscillation during awake-immobility and walking with the exception of power of low-frequency gamma of $VAChT^{Nkx2.1\text{-}Cre\text{-}flox/flox}$ mice during walking. This is consistent with the finding that AMPA receptor, but not NMDA blockade, in the hippocampus attenuated hippocampal gamma rhythm (Leung and Shen, 2004).

4.4 Limitations and future studies

While electrophysiology of the hippocampus of these two mutant mouse lines was studied during walking and awake-immobility, I did not study the hippocampal activation of these mice during sleep. LFPs recorded in this study were limited to the CA1 region of the hippocampus while it is important to record LFPs from other brain regions such as the neocortex. Efforts were made to select the best LFPs for each type of behavior; however, simultaneous video-LFP recording will significantly reduce the chance of errors made in this selection. Another major limitation in my study was proper placement of the electrodes as brain size varies from mouse to mouse. Using multi-channel electrodes will significantly increase the chance of placing electrodes into specific layer of the hippocampus, as well as provide laminar profiles of the LFPs. Cholinesterase inhibitor drugs such as galantamine are among the most common types of drugs used in controlling patients with AD. Since VAChT and acetylcholine deficient mice are models for AD, it is important to study the effects of these drugs on LFPs and behavior.

4.5 Conclusion

The availability of VAChT KD^{HET} and $VAChT^{Nkx2.1\text{-}Cre\text{-}flox/flox}$ mutant mouse lines displaying different levels of VAChT expression provides us with the unique opportunity to evaluate the consequences of reduced VAChT levels for brain functions. Multiple behavioral deficits such as social and object recognition, spatial memory, attention in the 5 choice serial reaction task and hyperactivity were observed in these genetically modified mice (Prado et al., 2006; Martin-Silva et al., 2011; Martyn et al., 2012: Al-Onaizi et al., under review). The primary goal of this study was to use electrophysiology to record LFPs from the hippocampus of these two mutant mouse lines in order to further define the role of VAChT and ACh release on hippocampal activation during awake-immobility and walking. The main findings of the present experiments are that (1) VAChT expression and ACh release are necessary for generation of hippocampal theta rhythm during awake-immobility, (2) generation of hippocampal theta rhythm during walking involved non-cholinergic neurotransmitters., although ACh was also involved (Leung, 1998); (3) gamma power in the hippocampus of VAChT KD^{HET} and $VAChT^{Nkx2.1\text{-}Cre\text{-}flox/flox}$ mice was not significantly different from that in Wild-Type mice, suggesting cholinergic neurons have little impact on generation of hippocampal gamma oscillations; (4) immobile theta in $VAChT^{Nkx2.1\text{-}Cre\text{-}flox/flox}$ and Wild-Type mice was sensitive to scopolamine, while VAChT KD^{HET} mice was not. Furthermore, VAChT KD^{HET} mice, as compared to Wild-Type mice, manifested higher peak theta frequency during walking. Cholinergic afferents from brainstem to septum may be compensated by non-cholinergic brainstem-septal synapses in VAChT KD^{HET} mice.

References

Allen, T. G., Abogadie, F. C., & Brown, D. A. (2006). Simultaneous release of glutamate and acetylcholine from single magnocellular "cholinergic" basal forebrain neurons. *The Journal of Neuroscience*, *26*(5), 1588-1595.

Alreja M, Wu M, Liu W, Atkins JB, Leranth C, Shanabrough M (2000). Muscarinic tone sustains impulse flow in the septohippocampal GABA but not cholinergic pathway: implications for learning and memory. *J Neurosci 20*, 8103-8110.

Al-Onaizi, M. A., Parfitt, G. M., Kolisnyk, B., Law, C. S. H., Martí Barros, D., Leung, L. W. S., Prado M. A., & Prado, V. F. Cholinergic regulation of hippocampal-dependent information processing: implications for Alzheimer's disease. *Under Review*

Amaral, D. G., & Kurz, J. (1985). An analysis of the origins of the cholinergic and noncholinergic septal projections to the hippocampal formation of the rat. *Journal of Comparative Neurology*, *240*(1), 37-59.

Amaral, D. G., & Witter, M. P. (1989). The three-dimensional organization of the hippocampal formation: a review of anatomical data. *Neuroscience*, *31*(3), 571-591.

Andersen, P., Bliss, T. V. P., & Skrede, K. K. (1971). Lamellar organization of hippocampal excitatory pathways. *Experimental Brain Research*, *13*(2), 222-238.

Balschun, D., Moechars, D., Callaerts-Vegh, Z., Vermaercke, B., Van Acker, N., Andries, L., & D'Hooge, R. (2010). Vesicular glutamate transporter VGLUT1 has a role in hippocampal long-term potentiation and spatial reversal learning. *Cerebral Cortex*, *20*(3), 684-693.

Bartus, R. T., Dean, R. L., Beer, B., & Lippa, A. S. (1982). The cholinergic hypothesis of geriatric memory dysfunction. *Science*, *217*(4558), 408-414.

Bassant, M. H., Apartis, E., Jazat-Poindessous, F. R., Wiley, R. G., & Lamour, Y. A. (1995). Selective immunolesion of the basal forebrain cholinergic neurons: effects on hippocampal activity during sleep and wakefulness in the rat. *Neurodegeneration*, *4*(1), 61-70.

Baxter, M. G., Bucci, D. J., Gorman, L. K., Wiley, R. G., & Gallagher, M. (2013). Selective immunotoxic lesions of basal forebrain cholinergic cells: effects on learning and memory in rats. *Behavioral Neuroscience*, *127*(5), 611-620.

Benes, F. M., & Berretta, S. (2001). GABAergic interneurons: implications for understanding schizophrenia and bipolar disorder. *Neuropsychopharmacology*, *25*(1), 1-27.

Bland, B. H. (1986). The physiology and pharmacology of hippocampal formation theta rhythms. *Progress in Neurobiology*, *26*(1), 1-54.

Bland, B. H., Jackson, J., Derrie-Gillespie, D., Azad, T., Rickhi, A., & Abriam, J. (2006). Amplitude, frequency, and phase analysis of hippocampal theta during sensorimotor processing in a jump avoidance task. *Hippocampus*, *16*(8), 673-681.

Bland, B. H., Konopacki, J., & Dyck, R. (2005). Heterogeneity among hippocampal pyramidal neurons revealed by their relation to theta-band oscillation and synchrony. *Experimental Neurology*, *195*(2), 458-474.

Bland, B. H., Trepel, C., Oddie, S. D., & Kirk, I. J. (1996). Intraseptal microinfusion of muscimol: effects on hippocampal formation theta field activity and phasic theta-ON cell discharges. *Experimental Neurology*, *138*(2), 286-297.

Bland, B. H., & Oddie, S. D. (2001). Theta band oscillation and synchrony in the hippocampal formation and associated structures: the case for its role in sensorimotor integration. *Behavioural Brain Research*, *127*(1), 119-136.

Bliss, T. V., & Collingridge, G. L. (1993). A synaptic model of memory: long-term potentiation in the hippocampus. *Nature*, *361*(6407), 31-39.

Bontempi B, Whelan KT, Risbrough VB, Rao TS, Buccafusco JJ, Lloyd GK, Menzaghi F (2001) SIB-1553A, (+/-)-4-[[2-(1-methyl-2-pyrrolidinyl)ethyl]thio]phenol hydrochloride, a subtype-selective ligand for nicotinic acetylcholine receptors with putative cognitive-enhancing properties: effects on working and reference memory performances in aged rodents and nonhuman primates. *The Journal of Pharmacology and Experimental Therapeutics,* 299:297-306.

Borhegyi, Z., Maglóczky, Z., Acsady, L., & Freund, T. F. (1997). The supramammillary nucleus innervates cholinergic and GABAergic neurons in the medial septum-diagonal band of Broca complex. *Neuroscience*, *82*(4), 1053-1065.

Bragin, A., Jandó, G., Nádasdy, Z., Hetke, J., Wise, K., & Buzsáki, G. (1995). Gamma (40-100 Hz) oscillation in the hippocampus of the behaving rat. *The Journal of Neuroscience*, *15*(1), 47-60.

Brun, V. H., Otnæss, M. K., Molden, S., Steffenach, H. A., Witter, M. P., Moser, M. B., & Moser, E. I. (2002). Place cells and place recognition maintained by direct entorhinal-hippocampal circuitry. *Science*, *296*(5576), 2243-2246.

Buzsáki, G. (2002). Theta oscillations in the hippocampus. *Neuron*, *33*(3), 325-340.

Buzsáki, G., Buhl, D. L., Harris, K. D., Csicsvari, J., Czeh, B., & Morozov, A. (2003). Hippocampal network patterns of activity in the mouse. *Neuroscience*, *116*(1), 201-211.

Chang, Q., & Gold, P. E. (2003). Switching memory systems during learning: changes in patterns of brain acetylcholine release in the hippocampus and striatum in rats. *The Journal of Neuroscience*, *23*(7), 3001-3005.

Charpak, S., Pare, D., & Llinas, R. (1995). The Entorhinal cortex entrains fast CA1 hippocampal oscillations in the anaesthetized guinea-pig: role of the monosynaptic component of the perforant path. *European Journal of Neuroscience*, *7*(7), 1548-1557.

Chuang, S. C., Bianchi, R., Kim, D., Shin, H. S., & Wong, R. K. (2001). Group I metabotropic glutamate receptors elicit epileptiform discharges in the hippocampus through PLCβ1 signaling. *The Journal of Neuroscience*, *21*(16), 6387-6394.

Chen, K. H., Reese, E. A., Kim, H. W., Rapoport, S. I., & Rao, J. S. (2011). Disturbed neurotransmitter transporter expression in Alzheimer's disease brain. *Journal of Alzheimer's Disease*, *26*(4), 755-766.

Cobb, S. R., & Davies, C. H. (2005). Cholinergic modulation of hippocampal cells and circuits. *The Journal of Physiology*, *562*(1), 81-88.

Coben, L. A., Danziger, W., & Storandt, M. (1985). A longitudinal EEG study of mild senile dementia of Alzheimer type: changes at 1 year and at 2.5 years. *Electroencephalography and Clinical Neurophysiology*, *61*(2), 101-112.

Colbert, C. M., & Levy, W. B. (1992). Electrophysiological and pharmacological characterization of perforant path synapses in CA1: mediation by glutamate receptors. *Journal of Neurophysiology*, *68*(1), 1-8.

Colgin, L. L., Denninger, T., Fyhn, M., Hafting, T., Bonnevie, T., Jensen, O., ... & Moser, E. I. (2009). Frequency of gamma oscillations routes flow of information in the hippocampus. *Nature*, *462*(7271), 353-357.

Colom, L. V., Castaneda, M. T., Reyna, T., Hernandez, S., & Garrido-sanabria, E. (2005). Characterization of medial septal glutamatergic neurons and their projection to the hippocampus. *Synapse*, *58*(3), 151-164.

Csicsvari, J., Jamieson, B., Wise, K. D., & Buzsáki, G. (2003). Mechanisms of gamma oscillations in the hippocampus of the behaving rat. *Neuron*, *37*(2), 311-322.

De Castro, B. M., Pereira, G. S., Magalhaes, V., Rossato, J. I., De Jaeger, X., Martins-Silva, C., ... & Prado, M. A. M. (2009). Reduced expression of the vesicular acetylcholine transporter causes learning deficits in mice. *Genes, Brain and Behavior*, *8*(1), 23-35.

Dewachter, I., Reversé, D., Caluwaerts, N., Ris, L., Kuipéri, C., Van den Haute, C., ... & Van Leuven, F. (2002). Neuronal deficiency of presenilin 1 inhibits amyloid plaque formation and corrects hippocampal long-term potentiation but not a cognitive defect of amyloid precursor protein [V717I] transgenic mice. *The Journal of Neuroscience*, *22*(9), 3445-3453.

Dobransky, T., & Rylett, R. J. (2005). A model for dynamic regulation of choline acetyltransferase by phosphorylation. *Journal of Neurochemistry*, *95*(2), 305-313.

Dudar, J., Whishaw, I. Q., & Szerb, J. C. (1979). Release of acetylcholine from the hippocampus of freely moving rats during sensory stimulation and running. *Neuropharmacology*, *18*(8), 673-678.

Eidelberg, E. (1982). Convergence of associational and commissural pathways on CA1 pyramidal cells of the rat hippocampus. *Brain Research*, *237*(2), 283-295.

Fabian-Fine, R., Skehel, P., Errington, M. L., Davies, H. A., Sher, E., Stewart, M. G., & Fine, A. (2001). Ultrastructural distribution of the α7 nicotinic acetylcholine receptor subunit in rat hippocampus. *The Journal of Neuroscience*, *21*(20), 7993-8003.

Fellous, J. M., & Sejnowski, T. J. (2000). Cholinergic induction of oscillations in the hippocampal slice in the slow(0. 5–2 Hz), theta(5–12 Hz), and gamma(35–70 Hz) bands. *Hippocampus*, *10*(2), 187-197.

Fisher, A. (2008). Cholinergic treatments with emphasis on m1 muscarinic agonists as potential disease-modifying agents for Alzheimer's disease. *Neurotherapeutics*, *5*(3), 433-442.

Francis, P. T., Palmer, A. M., Snape, M., & Wilcock, G. K. (1999). The cholinergic hypothesis of Alzheimer's disease: a review of progress. *Journal of Neurology, Neurosurgery & Psychiatry*, *66*(2), 137-147.

Freund, T. F., & Buzsáki, G. Y. (1996). Interneurons of the hippocampus. *Hippocampus*, *6*(4), 347-470.

Galey, D., Destrade, C., & Jaffard, R. (1994). Relationships between septo-hippocampal cholinergic activation and the improvement of long-term retention produced by medial septal electrial stimulation in two inbred strains of mice. *Behavioural Brain Research*, *60*(2), 183-189.

Gaykema, R., Luiten, P. G., Nyakas, C., & Traber, J. (1990). Cortical projection patterns of the medial septum-diagonal band complex. *Journal of Comparative Neurology*, *293*(1), 103-124.

Gillies, M. J., Traub, R. D., LeBeau, F. E. N., Davies, C. H., Gloveli, T., Buhl, E. H., & Whittington, M. A. (2002). A model of atropine-resistant theta oscillations in rat hippocampal area CA1. *The Journal of Physiology*, *543*(3), 779-793.

Green, J. D. (1964). The hippocampus. *Physiological Reviews*, *44*(4), 561-608.

Green, J. D., & Arduini, A. A. (1954). Hippocampal electrical activity in arousal. *Journal of Neurophysiology*, *17*, 531-557.

Goutagny, R., Jackson, J., & Williams, S. (2009). Self-generated theta oscillations in the hippocampus. *Nature Neuroscience*, *12*(12), 1491-1493.

Griffith, W. H. (1988). Membrane properties of cell types within guinea pig basal forebrain nuclei in vitro. *Journal of Neurophysiology*, *59*(5), 1590-1612.

Griffith, W. H., & Matthews, R. T. (1986). Electrophysiology of AChE-positive neurons in basal forebrain slices. *Neuroscience Letters*, *71*(2), 169-174.

Grover, L. M., & Teyler, T. J. (1990). Two components of long-term potentiation induced by different patterns of afferent activation. *Nature*, *347*(6292), 477-479.

Gu, Z., & Yekel, J. L. (2011). Timing-dependent septal cholinergic induction of dynamic hippocampal synaptic plasticity. *Neuron*, *71*(1), 155-165.

Hangya, B., Borhegyi, Z., Szilágyi, N., Freund, T. F., & Varga, V. (2009). GABAergic neurons of the medial septum lead the hippocampal network during theta activity. *The Journal of Neuroscience*, *29*(25), 8094-8102.

Hanse, E., & Gustafsson, B. (1994). TEA elicits two distinct potentiations of synaptic transmission in the CA1 region of the hippocampal slice. *The Journal of Neuroscience*, *14*(8), 5028-5034.

Hasselmo, M. E. (2005). What is the function of hippocampal theta rhythm?—Linking behavioral data to phasic properties of field potential and unit recording data. *Hippocampus*, *15*(7), 936-949.

Hasselmo, M. E. (2006). The role of acetylcholine in learning and memory. *Current Opinion in Neurobiology*, *16*(6), 710-715.

Harris, E. W., Ganong, A. H., & Cotman, C. W. (1984). Long-term potentiation in the hippocampus involves activation of N-methyl-D-aspartate receptors. *Brain Research*, *323*(1), 132-137.

Herreras, O., Solís, J. M., Herranz, A. S., Del Rio, R. M., & Lerma, J. (1988). Sensory modulation of hippocampal transmission. II. Evidence for a cholinergic locus of inhibition in the Schaffer-CA1 synapse. *Brain Research*, *461*(2), 303-313.

Heynen, A. J., & Bilkey, D. K. (1994). Effects of perforant path procaine on hippocampal type 2 rhythmical slow-wave activity (theta) in the urethane-anesthetized rat. *Hippocampus*, *4*(6), 683-695.

Hölscher, C., Anwyl, R., & Rowan, M. J. (1997). Stimulation on the positive phase of hippocampal theta rhythm induces long-term potentiation that can be depotentiated by stimulation on the negative phase in area CA1 in vivo. *The Journal of Neuroscience*, *17*(16), 6470-6477.

Hu, H., Vervaeke, K., Graham, L. J., & Storm, J. F. (2009). Complementary theta resonance filtering by two spatially segregated mechanisms in CA1 hippocampal pyramidal neurons. *The Journal of Neuroscience*, *29*(46), 14472-14483.

Huh, C. Y., Goutagny, R., & Williams, S. (2010). Glutamatergic neurons of the mouse medial septum and diagonal band of Broca synaptically drive hippocampal pyramidal cells: relevance for hippocampal theta rhythm. *The Journal of Neuroscience*, *30*(47), 15951-15961.

Hyman, J. M., Wyble, B. P., Goyal, V., Rossi, C. A., & Hasselmo, M. E. (2003). Stimulation in hippocampal region CA1 in behaving rats yields long-term potentiation when delivered to the peak of theta and long-term depression when delivered to the trough. *The Journal of Neuroscience*, *23*(37), 11725-11731.

Ji, D., Lape, R., & Dani, J. A. (2001). Timing and location of nicotinic activity enhances or depresses hippocampal synaptic plasticity. *Neuron*, *31*(1), 131-141.

Kashani, A., Betancur, C., Giros, B., Hirsch, E., & El Mestikawy, S. (2007). Altered expression of vesicular glutamate transporters VGLUT1 and VGLUT2 in Parkinson disease. *Neurobiology of Aging*, *28*(4), 568-578.

Kirk, I. J. (1998). Frequency modulation of hippocampal theta by the supramammillary nucleus, and other hypothalamo–hippocampal interactions: mechanisms and functional implications. *Neuroscience & Biobehavioral Reviews*, *22*(2), 291-302.

Kirvell, S. L., Esiri, M., & Francis, P. T. (2006). Down-regulation of vesicular glutamate transporters precedes cell loss and pathology in Alzheimer's disease. *Journal of Neurochemistry*, *98*(3), 939-950.

Kiss, J., Csaki, A., Bokor, H., Shanabrough, M., & Leranth, C. (2000). The supramammillo-hippocampal and supramammillo-septal glutamatergic/aspartatergic projections in the rat: a combined [^{3}H] d-aspartate autoradiographic and immunohistochemical study. *Neuroscience, 97*(4), 657-669.

Kiss, J., Csaki, A., Bokor, H., Kocsis, K., & Kocsis, B. (2002). Possible glutamatergic/aspartatergic projections to the supramammillary nucleus and their origins in the rat studied by selective [^{3}H] D-aspartate labelling and immunocytochemistry. *Neuroscience*, *111*(3), 671-691.

Klausberger, T., & Somogyi, P. (2008). Neuronal diversity and temporal dynamics: the unity of hippocampal circuit operations. *Science*, *321*(5885), 53-57.

Knapp, J. A., Morris, N. P., Henderson, Z., & Matthews, R. T. (2000). Electrophysiological characteristics of non-bursting, glutamate decarboxylase messenger RNA-positive neurons of the medial septum/diagonal band nuclei of guinea-pig and rat. *Neuroscience*, *98*(4), 661-668.

Knowles, W. D. (1992). Normal anatomy and neurophysiology of the hippocampal formation. *Journal of Clinical Neurophysiology*, *9*(2), 253-263.

Konopacki, J., MacIver, M. B., Bland, B. H., & Roth, S. H. (1987). Carbachol-induced EEG 'theta'activity in hippocampal brain slices. *Brain Research*, *405*(1), 196-198.

Kocsis, B., Bragin, A., & Buzsáki, G. (1999). Interdependence of multiple theta generators in the hippocampus: a partial coherence analysis. *The Journal of Neuroscience*, *19*(14), 6200-6212.

Lanzafame, A. A., Christopoulos, A., & Mitchelson, F. (2003). Cellular signaling mechanisms for muscarinic acetylcholine receptors. *Receptors and Channels*, *9*(4), 241-260.

Larson, J., Wong, D., & Lynch, G. (1986). Patterned stimulation at the theta frequency is optimal for the induction of hippocampal long-term potentiation. *Brain Research*, *368*(2), 347-350.

Lawson, V. H., & Bland, B. H. (1993). The role of the septohippocampal pathway in the regulation of hippocampal field activity and behavior: analysis by the intraseptal microinfusion of carbachol, atropine, and procaine. *Experimental Neurology*, *120*(1), 132-144.

Lee, M. G., Chrobak, J. J., Sik, A., Wiley, R. G., & Buzsaki, G. (1994). Hippocampal theta activity following selective lesion of the septal cholinergic system. *Neuroscience*, *62*(4), 1033-1047.

Lee, M. G., Hassani, O. K., Alonso, A., & Jones, B. E. (2005). Cholinergic basal forebrain neurons burst with theta during waking and paradoxical sleep. *The Journal of Neuroscience*, *25*(17), 4365-4369.

Leung, L. S. (1982). Nonlinear feedback model of neuronal populations in hippocampal CAl region. *Journal of Neurophysiology*, *47*(5), 845-868.

Leung, L. W. (1984). Model of gradual phase shift of theta rhythm in the rat. *Journal of Neurophysiology*, *52*(6), 1051-1065.

Leung, L. W. S. (1985). Spectral analysis of hippocampal EEG in the freely moving rat: effects of centrally active drugs and relations to evoked potentials. *Electroencephalography and Clinical Neurophysiology*, *60*(1), 65-77.

Leung, L. S. (1998). Generation of theta and gamma rhythms in the hippocampus. *Neuroscience & Biobehavioral Reviews*, *22*(2), 275-290.

Leung, L. W. S., Da Silva, F. L., & Wadman, W. J. (1982). Spectral characteristics of the hippocampal EEG in the freely moving rat. *Electroencephalography and Clinical Neurophysiology*, *54*(2), 203-219.

Leung, L. S., Petropoulos, S., Shen, B., Luo, T., Herrick, I., Rajakumar, N., & Ma, J. (2011). Lesion of cholinergic neurons in nucleus basalis enhances response to general anesthetics. *Experimental Neurology*, *228*(2), 259-269.

Leung, L. W. S., & Desborough, K. A. (1988). APV, an N-methyl-D-aspartate receptor antagonist, blocks the hippocampal theta rhythm in behaving rats. *Brain Research*, *463*(1), 148-152.

Leung, L. S., & Shen, B. (1999). N-methyl-D-aspartate receptor antagonists are less effective in blocking long-term potentiation at apical than basal dendrites in hippocampal CA1 of awake rats. *Hippocampus*, *9*(6), 617-630.

Leung, L. S., & Shen, B. (2004). Glutamatergic synaptic transmission participates in generating the hippocampal EEG. *Hippocampus*, *14*(4), 510-525.

Leung, L. W. S., & Yim, C. Y. C. (1991). Intrinsic membrane potential oscillations in hippocampal neurons in vitro. *Brain Research*, *553*(2), 261-274.

Leung, L. S., Shen, B., Rajakumar, N., & Ma, J. (2003). Cholinergic activity enhances hippocampal long-term potentiation in CA1 during walking in rats. *The Journal of Neuroscience*, *23*(28), 9297-9304.

Levey, A. I., Edmunds, S. M., Koliatsos, V., Wiley, R. G., & Heilman, C. J. (1995). Expression of m1-m4 muscarinic acetylcholine receptor proteins in rat hippocampus and regulation by cholinergic innervation. *The Journal of Neuroscience*, *15*(5), 4077-4092.

Macadar, A. W., Chalupa, L. M., & Lindsley, D. B. (1974). Differentiation of brain stem loci which affect hippocampal and neocortical electrical activity. *Experimental Neurology*, *43*(3), 499-514.

Malenka, R. C., Kauer, J. A., Zucker, R. S., & Nicoll, R. A. (1988). Postsynaptic calcium is sufficient for potentiation of hippocampal synaptic transmission. *Science*, *242*(4875), 81-84.

Malenka, R. C., & Nicoll, R. A. (1993). NMDA-receptor-dependent synaptic plasticity: multiple forms and mechanisms. *Trends in Neurosciences*, *16*(12), 521-527.

Manns, I. D., Alonso, A., & Jones, B. E. (2003). Rhythmically discharging basal forebrain units comprise cholinergic, GABAergic, and putative glutamatergic cells. *Journal of Neurophysiology*, *89*(2), 1057-1066.

Markram, H., & Segal, M. (1990). Acetylcholine potentiates responses to N-methyl-D-aspartate in the rat hippocampus. *Neuroscience Letters*, *113*(1), 62-65.

Martins-Silva, C., De Jaeger, X., Guzman, M. S., Lima, R. D., Santos, M. S., Kushmerick, C., ... & Prado, V. F. (2011). Novel strains of mice deficient for the vesicular acetylcholine transporter: insights on transcriptional regulation and control of locomotor behavior. *PLoS One*, *6*(3), e17611.

Martyn, A. C., De Jaeger, X., Magalhães, A. C., Kesarwani, R., Gonçalves, D. F., Raulic, S., ... & Prado, V. F. (2012). Elimination of the vesicular acetylcholine transporter in the forebrain causes hyperactivity and deficits in spatial memory and long-term potentiation. *Proceedings of the National Academy of Sciences*, *109*(43), 17651-17656.

McKinney, M., Coyle, J. T., & Hedreen, J. C. (1983). Topographic analysis of the innervation of the rat neocortex and hippocampus by the basal forebrain cholinergic system. *Journal of Comparative Neurology*, *217*(1), 103-121.

Meldrum, B. S. (2000). Glutamate as a neurotransmitter in the brain: review of physiology and pathology. *The Journal of Nutrition*, *130*(4), 1007S-1015S.

Miyazaki, T., Fukaya, M., Shimizu, H., & Watanabe, M. (2003). Subtype switching of vesicular glutamate transporters at parallel fibre–Purkinje cell synapses in developing mouse cerebellum. *European Journal of Neuroscience*, *17*(12), 2563-2572.

Montgomery, S. M., & Buzsáki, G. (2007). Gamma oscillations dynamically couple hippocampal CA3 and CA1 regions during memory task performance. *Proceedings of the National Academy of Sciences*, *104*(36), 14495-14500.

Morris, N. P., Harris, S. J., & Henderson, Z. (1999). Parvalbumin-immunoreactive, fast-spiking neurons in the medial septum/diagonal band complex of the rat: intracellular recordings in vitro. *Neuroscience*, *92*(2), 589-600.

Moutsimilli, L., Farley, S., Dumas, S., El Mestikawy, S., Giros, B., & Tzavara, E. T. (2005). Selective cortical VGLUT1 increase as a marker for antidepressant activity. *Neuropharmacology*, *49*(6), 890-900.

Nitsch, R., & Leranth, C. (1996). GABAergic neurons in the rat dentate gyrus are innervated by subcortical calretinin-containing afferents. *Journal of Comparative Neurology*, *364*(3), 425-438.

Oddie, S. D., Bland, B. H., Colom, L. V., & Vertes, R. P. (1994). The midline posterior hypothalamic region comprises a critical part of the ascending brainstem hippocampal synchronizing pathway. *Hippocampus*, *4*(4), 454-473.

Oddie, S. D., & Bland, B. H. (1998). Hippocampal formation theta activity and movement selection. *Neuroscience & Biobehavioral Reviews*, *22*(2), 221-231.

Ovsepian, S. V., Anwyl, R., & Rowan, M. J. (2004). Endogenous acetylcholine lowers the threshold for long-term potentiation induction in the CA1 area through muscarinic receptor activation: in vivo study. *European Journal of Neuroscience*, *20*(5), 1267-1275.

Parent, M. B., & Baxter, M. G. (2004). Septohippocampal acetylcholine: involved in but not necessary for learning and memory?. *Learning & Memory*, *11*(1), 9-20.

Parsons, S. M. (2000). Transport mechanisms in acetylcholine and monoamine storage. *The FASEB Journal*, *14*(15), 2423-2434.

Patel, J. C., Rossignol, E., Rice, M. E., & Machold, R. P. (2012). Opposing regulation of dopaminergic activity and exploratory motor behavior by forebrain and brainstem cholinergic circuits. *Nature Communications*, *3*, 1172-1181.

Penttonen, M., Kamondi, A., Acsády, L., & Buzsáki, G. (1998). Gamma frequency oscillation in the hippocampus of the rat: intracellular analysis in vivo. *European Journal of Neuroscience*, *10*(2), 718-728.

Phillis, J. W. (2005). Acetylcholine release from the central nervous system: a 50-year retrospective. *Critical Reviews in Neurobiology*, *17*(3-4), 161-217.

Prado, V. F., Martins-Silva, C., de Castro, B. M., Lima, R. F., Barros, D. M., Amaral, E., ... & Prado, M. A. (2006). Mice deficient for the vesicular acetylcholine transporter are myasthenic and have deficits in object and social recognition. *Neuron*, *51*(5), 601-612.

Prediger, R. D., De-Mello, N., & Takahashi, R. N. (2006). Pilocarpine improves olfactory discrimination and social recognition memory deficits in 24 month-old rats. *European Journal of Pharmacology*, *531*(1), 176-182.

Ranck, J. B. (1973). Studies on single neurons in dorsal hippocampal formation and septum in unrestrained rats: Part I. Behavioral correlates and firing repertoires. *Experimental Neurology*, *41*(2), 462-531.

Rasmusson, D. D. (2000). The role of acetylcholine in cortical synaptic plasticity. *Behavioural Bain Research*, *115*(2), 205-218.

Roghani, A., Feldman, J., Kohan, S. A., Shirzadi, A., Gundersen, C. B., Brecha, N., & Edwards, R. H. (1994). Molecular cloning of a putative vesicular transporter for acetylcholine. *Proceedings of the National Academy of Sciences*, *91*(22), 10620-10624.

Rouse, S. T., Marino, M. J., Potter, L. T., Conn, P. J., & Levey, A. I. (1999). Muscarinic receptor subtypes involved in hippocampal circuits. *Life Sciences*, *64*(6), 501-509.

Sainsbury, R. S., Heynen, A., & Montoya, C. P. (1987). Behavioral correlates of hippocampal type 2 theta in the rat. *Physiology & Behavior*, *39*(4), 513-519.

Schliebs, R., & Arendt, T. (2006). The significance of the cholinergic system in the brain during aging and in Alzheimer's disease. *Journal of Neural Transmission*, *113*(11), 1625-1644.

Sederberg, P. B., Schulze-Bonhage, A., Madsen, J. R., Bromfield, E. B., McCarthy, D. C., Brandt, A., ... & Kahana, M. J. (2007). Hippocampal and neocortical gamma oscillations predict memory formation in humans. *Cerebral Cortex*, *17*(5), 1190-1196.

Serafin, M., Williams, S., Khateb, A., Fort, P., & Mühlethaler, M. (1996). Rhythmic firing of medial septum non-cholinergic neurons. *Neuroscience*, *75*(3), 671-675.

Shin, J., Kim, D., Bianchi, R., Wong, R. K., & Shin, H. S. (2005). Genetic dissection of theta rhythm heterogeneity in mice. *Proceedings of the National Academy of Sciences of the United States of America*, *102*(50), 18165-18170.

Simon, A. P., Poindessous-Jazat, F., Dutar, P., Epelbaum, J., & Bassant, M. H. (2006). Firing properties of anatomically identified neurons in the medial septum of anesthetized and unanesthetized restrained rats. *The Journal of Neuroscience*, *26*(35), 9038-9046.

Sotty, F., Danik, M., Manseau, F., Laplante, F., Quirion, R., & Williams, S. (2003). Distinct electrophysiological properties of glutamatergic, cholinergic and GABAergic rat septohippocampal neurons: novel implications for hippocampal rhythmicity. *The Journal of Physiology*, *551*(3), 927-943.

Stewart M, Fox SE (1989). Two populations of rhythmically bursting neurons in rat medial septum are revealed by atropine. *Journal of Neurophysiology 61*, 982-993.

Stewart, M., & Fox, S. E. (1990). Do septal neurons pace the hippocampal theta rhythm?. *Trends in neurosciences*, *13*(5), 163-169.

Stumpf, C. (1965a). Drug action on the electrical activity of the hippocampus. *International Review of Neurobiology*, *8*, 77-138.

Stumpf, C. (1965b). The fast component in the electrical activity of rabbit's hippocampus. *Electroencephalography and Clinical Neurophysiology*. *18*, 477-486.

Tai, S. K., Ma, J., Ossenkopp, K. P., & Leung, L. S. (2012). Activation of immobility-related hippocampal theta by cholinergic septohippocampal neurons during vestibular stimulation. *Hippocampus*, *22*(4), 914-925.

Takács, V. T., Klausberger, T., Somogyi, P., Freund, T. F., & Gulyás, A. I. (2012). Extrinsic and local glutamatergic inputs of the rat hippocampal CA1 area differentially innervate pyramidal cells and interneurons. *Hippocampus*,*22*(6), 1379-1391.

Teipel, S. J., Flatz, W. H., Heinsen, H., Bokde, A. L., Schoenberg, S. O., Stöckel, S., ... & Hampel, H. (2005). Measurement of basal forebrain atrophy in Alzheimer's disease using MRI. *Brain*, *128*(11), 2626-2644.

Tordera, R. M., Totterdell, S., Wojcik, S. M., Brose, N., Elizalde, N., Lasheras, B., & Del Rio, J. (2007). Enhanced anxiety, depressive-like behaviour and impaired recognition memory in mice with reduced expression of the vesicular glutamate transporter 1 (VGLUT1). *European Journal of Neuroscience*, *25*(1), 281-290.

Tort, A. B., Komorowski, R. W., Manns, J. R., Kopell, N. J., & Eichenbaum, H. (2009). Theta–gamma coupling increases during the learning of item–context associations. *Proceedings of the National Academy of Sciences*, *106*(49), 20942-20947.

Tukker, J. J., Fuentealba, P., Hartwich, K., Somogyi, P., & Klausberger, T. (2007). Cell type-specific tuning of hippocampal interneuron firing during gamma oscillations in vivo. *The Journal of Neuroscience*, *27*(31), 8184-8189.

Vandecasteele, M., Varga, V., Berényi, A., Papp, E., Barthó, P., Venance, L., ... & Buzsáki, G. (2014). Optogenetic activation of septal cholinergic neurons suppresses sharp wave ripples and enhances theta oscillations in the hippocampus. *Proceedings of the National Academy of Sciences*, *111*(37), 13535-13540.

Vanderwolf, C. H. (1969). Hippocampal electrical activity and voluntary movement in the rat. *Electroencephalography and Cinical Neurophysiology*,*26*(4), 407-418.

Vanderwolf, C. H. (1975). Neocortical and hippocampal activation in relation to behavior: Effects of atropine, eserine, phenothiazines, and amphetamine. *Journal of Comparative and Physiological Psychology*, *88*(1), 300-323.

Vanderwolf, C. H. (1988). Cerebral activity and behavior: control by central cholinergic and serotonergic systems. *International Review of Neurobiology*, *30*, 225-340.

Vanderwolf, C. H., Buzsaki, G., Cain, D. P., Cooley, R. K., & Robertson, B. (1988). Neocortical and hippocampal electrical activity following decapitation in the rat. *Brain Research*, *451*(1), 340-344.

Vanderwolf, C. H., & Leung, L. W. S. (1983). Hippocampal rhythmical slow activity: A brief history and the effects of entorhinal lesions and phencyclidine. *Neurobiology of the Hippocampus*, 275.

Vertes, R. P. (1981). An analysis of ascending brain stem systems involved in hippocampal synchronization and desynchronization. *Journal of Neurophysiology*, *46*(5), 1140-1159.

Vertes, R. P. (1982). Brain stem generation of the hippocampal EEG. *Progress in Neurobiology*, *19*(3), 159-186.

Vertes, R. P. (1992). PHA-L analysis of projections from the supramammillary nucleus in the rat. *Journal of Comparative Neurology*, *326*(4), 595-622.

Vertes, R. P., & Kocsis, B. (1997). Brainstem-diencephalo-septohippocampal systems controlling the theta rhythm of the hippocampus. *Neuroscience*, *81*(4), 893-926.

Volpicelli, L. A., & Levey, A. I. (2004). Muscarinic acetylcholine receptor subtypes in cerebral cortex and hippocampus. *Progress in Brain Research*, *145*, 59-66.

Winson, J. (1978). Loss of hippocampal theta rhythm results in spatial memory deficit in the rat. *Science*, *201*(4351), 160-163.

Wolansky, T., Clement, E. A., Peters, S. R., Palczak, M. A., & Dickson, C. T. (2006). Hippocampal slow oscillation: a novel EEG state and its coordination with ongoing neocortical activity. *The Journal of Neuroscience*, *26*(23), 6213-6229.

Wu, M., Shanabrough, M., Leranth, C., & Alreja, M. (2000). Cholinergic excitation of septohippocampal GABA but not cholinergic neurons: implications for learning and memory. *The Journal of Neuroscience*, *20*(10), 3900-3908.

Wu, C. K., Thal, L., Pizzo, D., Hansen, L., Masliah, E., & Geula, C. (2005). Apoptotic signals within the basal forebrain cholinergic neurons in Alzheimer's disease. *Experimental Neurology*, *195*(2), 484-496.

Wyss, J. M., Swanson, L. W., & Cowan, W. M. (1979). A study of subcortical afferents to the hippocampal formation in the rat. *Neuroscience*, *4*(4), 463-476.

Xu, Q., Tam, M., & Anderson, S. A. (2008). Fate mapping Nkx2. 1-lineage cells in the mouse telencephalon. *Journal of Comparative Neurology*, *506*(1), 16-29.

Yoder, R. M., & Pang, K. C. (2005). Involvement of GABAergic and cholinergic medial septal neurons in hippocampal theta rhythm. *Hippocampus*, *15*(3), 381-392.

Zalutsky, R. A., & Nicoll, R. A. (1990). Comparison of two forms of long-term potentiation in single hippocampal neurons. *Science*, *248*(4963), 1619-1624.

Curriculum Vitae

Name: Shahin Moallem

Post-secondary Education and Degrees:

University of Toronto, Scarborough
Toronto, Ontario, Canada
Human Biology Specialist
Honours Bachelor of Science
2007-2012

The University of Western Ontario
London, Ontario, Canada
Master's of Science
Neuroscience
2013-2015

Honours and Awards:

Western Graduate Research Scholarship
2013-2015

In-Course Scholarship
University of Toronto, Scarborough
2011-2012

Honors List, Third Year
University of Toronto, Scarborough
2011

Honors List, Forth Year
University of Toronto, Scarborough
2012

Related Work Experience:

Teaching Assistant
Department of Psychology,
The University of Western Ontario
2013-2014
Dr. M. Atkinson, Psychology 1000

Teaching Assistant
Department of Neuroscience,
Schulich School of Medicine and Dentistry,
The University of Western Ontario
2014-2015
Dr. A. Brown, Neuroscience 9550

Conferences and Presentations:

London Health Research Day
London, Ontario
Abnormal Hippocampal Activation In Freely Behaving Mice Deficient For The Vesicular Acetylcholine Transporter (Poster Presentation)
April 2015

Society for Neuroscience (SfN)
Washington, DC, USA
Abnormal Hippocampal Activation In Freely Behaving Mice Deficient For The Vesicular Acetylcholine Transporter (Poster Presentation)
November 2014

Southern Ontario Neuroscience Association (SONA)
London, Ontario
Abnormal Hippocampal Activation In Freely Behaving Mice Deficient For The Vesicular Acetylcholine Transporter (Poster Presentation)
May 2014

Society for Neuroscience (SfN)
San Diego, CA, USA
(Conference Attendee)
November 2013

Volunteer Activities:

Research Assistant
University of Toronto, Scarborough
Animal Physiology
2012
Dr. Kenneth Welch

Supervised Study
University of Toronto, Scarborough
Biodiversity and Ecosystem Functioning
2011
Dr. Marc Cadotte

Clinical Observer
Dawes Road Dental Clinic
2011
Dr. Ali Shekari